Back-arc dynamics controlled by slab rollback and tearing: a reappraisal of seafloor spreading and kinematic evolution of the Eastern Algerian basin (western Mediterranean) in Middle-Late Miocene

Shaza Haidar[1], Jacques Déverchère[1], David Graindorge[1], Mohamed Arab[2], Mourad Medaouri[2], and Frauke Klingelhoefer[3]

[1]Université de Bretagne Occidentale - Institut Universitaire Européen de la Mer
[2]SONATRACH, Division Exploration
[3]IFREMER

November 22, 2022

Abstract

In spite of clear fan-shaped magnetic anomalies in the Eastern Algerian Basin (EAB), the way how and the time when seafloor spreading occurred are still debated. In this work, a new seismo-stratigraphic interpretation based on deep-penetration reflection seismic data correlated to reduced-to-the-pole magnetic anomalies and to onshore-offshore litho-stratigraphic correlation of Pre-Messinian units bring new constraints on its age and mode of opening. Our results reveal that the seafloor spreading of EAB occurred with a intermediate to fast half-spreading rate of 3.7±0.5 cm/yr during 2.45±0.18 Myr in Langhian-Serravalian times, i.e. after the Corsica-Sardinia block rotation and the collision of Lesser Kabylia with Africa. We revise the kinematics of the Algero-Balearic domain into three stages: (1) birth of a highly stretched continental basin accommodating the southern drift of the Kabylies driven by Tethyan slab rollback between ˜23 and ˜15 Ma, (2) fast opening of a new basin (EAB) between 15.2 and 12.7 Ma by clockwise rotation of a Greater Alboran Block (GALB), and (3) continuation of westward translation of the GALB. The last stages match both the late formation of Subduction-Transform Edge Propagator (STEP) faults at the toes of the Algero-Balearic margins and the post-collisional volcanic migration along the Algerian margin interpreted as related to slab break-off. This new scheme invalidates most previous opening models of the Algero-Balearic basin and favors a significant stretching and splitting of the GALB into several continental fragments resulting from the westward propagation of the arcuate subduction front by lateral tearing of a narrow slab.

Back-arc dynamics controlled by slab rollback and tearing: a reappraisal of seafloor spreading and kinematic evolution of the Eastern Algerian basin (western Mediterranean) in Middle-Late Miocene

Shaza Haidar[1*], Jacques Déverchère[1], David Graindorge[1], Mohamed Arab[2], Mourad Medaouri[2], Frauke Klingelhoefer[3]

[1] Univ. Brest, CNRS, Laboratoire Géosciences Océan, 29280 Plouzané, France.

[2] SONATRACH, Division Exploration, 3029 Boumerdes, Algeria.

[3] IFREMER, Géosciences Marines, Centre de Brest, 29280 Plouzané, France.

Corresponding author: Shaza Haidar (shaza.haidar@univ-brest.fr)

Key Points:

- New seismo-stratigraphic interpretation of pre-Messinian units and analysis of a reduced-to-the-pole magnetic anomaly pattern of the Eastern Algerian basin
- Reassessment of the proposed kinematic reconstructions of the Algero-Balearic basin and building of a semiquantitative model during Middle-Late Miocene
- A combination of Tethyan slab rollback and slab tearing explains fast rotation, translation and fragmentation of the fore-arc after collision of the Kabylies

Abstract

In spite of clear fan-shaped magnetic anomalies in the Eastern Algerian Basin (EAB), the way how and the time when seafloor spreading occurred are still debated. In this work, a new seismo-stratigraphic interpretation based on deep-penetration reflection seismic data correlated to reduced-to-the-pole magnetic anomalies and to onshore-offshore litho-stratigraphic correlation of Pre-Messinian units bring new constraints on its age and mode of opening. Our results reveal that the seafloor spreading of EAB occurred with a intermediate to fast half-spreading rate of 3.7±0.5 cm/yr during 2.45±0.18 Myr in Langhian-Serravalian times, i.e. after the Corsica-Sardinia block rotation and the collision of Lesser Kabylia with Africa. We revise the kinematics of the Algero-Balearic domain into three stages: (1) birth of a highly stretched continental basin accommodating the southern drift of the Kabylies driven by Tethyan slab rollback between ~23 and ~15 Ma, (2) fast opening of a new basin (EAB) between 15.2 and 12.7 Ma by clockwise rotation of a Greater Alboran Block (GALB), and (3) continuation of westward translation of the GALB. The last stages match both the late formation of Subduction-Transform Edge Propagator (STEP) faults at the toes of the Algero-Balearic margins and the post-collisional volcanic migration along the Algerian margin interpreted as related to slab break-off. This new scheme invalidates most previous opening models of the Algero-Balearic basin and favors a significant stretching and splitting of the GALB into several continental fragments resulting from the westward propagation of the arcuate subduction front by lateral tearing of a narrow slab.

1 Introduction

The Western Mediterranean Sea is a complex geological domain that has received much attention since the early 1970s. Several kinematic and geodynamic models have been proposed to explain the coeval birth and growth of orogenic belts (Rif-Betic cordillera, Maghrebides, Alps, Apennines, Dinarides) and extensional basins (Alboran, Algerian, Valencia, Liguro-Provençal, Tyrrhenian) in the frame of a NW-SE plate convergence of Africa with respect to Eurasia since 35 Ma (e.g., Alvarez et al., 1974; Biju-Duval et al., 1977; Cohen, 1980; Dewey et al., 1989, 1973) (Figure 1).

There is today a consensus to consider that the rollback of subducted slab segments is the driving mechanism in the tectonic evolution of the Western Mediderranean sea, explaining the collapse of mountain belts and the development of extension in the upper plate as soon as slab retreat initiates and migrates by following the backward motion of the trench (e.g., Dewey et al., 1989; Jolivet and Faccenna, 2000; Lonergan and White, 1997; Malinverno and Ryan, 1986; Rehault et al., 1984; Wortel and Spakman, 2001). However, the rollback schemes proposed since 20 years display strikingly different subduction geometries. They can be summarized as follows: (1) single, continuous trench retreat along the entire Gibraltar-Balearic system (Gueguen et al., 1998; Faccenna et al., 2004; Jolivet et al., 2009); (2) initial subduction south of the Balearic Islands, with a southward trench migration turning westward later on (Rosenbaum et al., 2002; Spakman and Wortel, 2004; van Hinsbergen et al., 2014); and (3) opposite vergence of two subduction systems of variable size and geometry migrating in opposite directions (Michard et al., 2002; Gelabert et al., 2002; Vergés and Fernàndez, 2012; Leprêtre et al., 2018; Romagny et al., 2020). These contrasting models often result from different interpretations of seismic tomography where high velocity anomalies are assumed to represent remnants of subducted slab fragments (Carminati et al., 1998a,b; Fichtner and Villaseñor, 2015; Piromallo and Morelli, 2003; Spakman and Wortel, 2004).

In the northern part of the Western and Central Mediterranean, the kinematic evolution of sub-basins is well established thanks to a large number of regional studies based on analyses of seismic and borehole data, paleomagnetic studies, on-offshore geological correlations or geochemical sampling. This is indeed the case for the Liguro-Provençal basin (Gueguen et al., 1998; Rehault et al., 1984) where extension started in the Upper Oligocene owing to NW-SE-directed Tethyan slab retreat and ended after the counterclockwise rotation of the Corsica-Sardinia block at ~ 15-16 Ma (Gattacceca et al., 2007; Speranza et al., 2002). The neighbouring intra-continental Valencia trough is floored by thinned continental crust, representing an aborted rift (Maillard et al., 1992; Roca and Guimerà, 1992; Ayala et al., 2016; Pellen et al., 2016). In the central Mediterranean domain, the opening of the Tyrrhenian basin has started in late Miocene as a result of the south-east retreat of the Calabrian slab (Carminati et al., 1998a,b; Guillaume et al., 2010; Jolivet and Faccenna, 2000; Malinverno and Ryan, 1986). By contrast, the kinematic evolution of the Alboran and Algero-Balearic domains remains debated, with three main scenarios generally proposed: i) fast and large (>600 km) westward motion of a rigid continental block (Andrieux et al., 1971; Mauffret et al., 2004); ii) delamination process with almost no displacement of the Alboran block (Platt and Vissers, 1989; Platt et al., 2006); iii) coeval opening of the Algero-Balearic (AB) and Liguro-Provençal (LP) basins followed by moderate westward motion of the Alboran plate driven by rollback of the Gibraltar subduction slab (Lonergan and White, 1997; Royden, 1993; Spakman and Wortel, 2004). Although slab rollback, detachment and tearing is generally accepted as the driving force, many questions remain unsolved, in particular the paleogeography and geometry of the Alboran and Balearic domains, their internal paleo-deformation, as well as the nature of the crust and the age of the Algero-Balearic (AB) basin.

In this work, we aim to build an updated, semi-quantitative kinematic model of the AB basin by focusing on the history of the Eastern Algerian basin (EAB). By contrast with previous reconstructions, we attempt to perform a tight spatio-temporal correlation of paleomagnetic anomalies and seismic reflection data in the entire EAB. To address this issue, we build an age model of the first pre-Messinian seismo-stratigraphic units overlying the oceanic crust, concurrently correlated with (1) magnetic stripes in the well-identified “sphenochasm”-shaped zone of the EAB (Carey, 1955), (2) paleobathymetry of the oceanic basement and (3) geological evidence of sedimentation and magmatism on the East Algerian margin (Lesser Kabylia). The constraints brought here allow us to propose a new scenario of opening of the AB basin and of the tectonic history of the Alboran domain.

2 Geological setting and kinematic models

2.1 Paleogeographic and plate tectonic settings

The basins of the western Mediterranean Sea are considered as back-arc extensional basins formed by the rollback of the Tethyan slab during Oligo-Miocene times (Frizon de Lamotte et al., 2000; Jolivet and Faccenna, 2000; Malinverno and Ryan, 1986); and references therein) south of the European plate, defining a segmented forearc known as the AlKaPeCa domain for Alboran (Al: internal Betics and Rif), Kabylian (Ka), Peloritani (Pe) and Calabria (Ca) terranes, respectively (Bouillin, 1986). This evolution was marked by sporadic volcanism displaying a fairly clear migration of arc magmatism (calco-alkaline) from the LP basin during Oligocene to the Alboran domain during upper Miocene (Carminati et al., 2012). The main pending questions in the western Mediterranean Sea remain when and how the Algero-Balearic Basin (AB) opened.

This basin is separated from the LP basin to the north by the North Balearic Fracture Zone (NBFZ) which played a key role in the basin opening as a "swinging door" (Martin, 2006). It is limited by the North African margin to the south, the Alboran basin to the west, and the western margin of Sardinian and Tunisian margins to the east (Figure 1). The western and central oceanic domains of the AB basin are bordered by different types of margins, considered as being either of transform or rifted types (Badji et al., 2015; Bouyahiaoui et al., 2015; Govers and Wortel, 2005; Maillard et al., 2020; Medaouri et al., 2014; van Hinsbergen et al., 2014 and references therein). The Lesser Kabylia (LK) block displays (1) a collision zone (south) and (2) a passive-type margin (north) bearing the oldest sedimentary units identified off Algeria and evidencing a SE-ward drift of the block (Arab et al., 2016b). However, its motion before collision with Africa 19 Myr ago follows quite different directions ranging from N-S to E-W, depending on assumptions made (e.g., Cohen, 1980; Driussi et al., 2015; Martin, 2006; Mauffret et al., 2004; Platt et al., 2013; Schettino and Turco, 2006), thus questioning its kinematic history relative to the EAB.

Marine magnetic anomalies are key proxies to constrain the oceanic seafloor ages, spreading directions and spreading rates (Vine and Matthews, 1963). However, the western Mediterranean Sea only displays patches of magnetic lineations within large areas of irregular anomaly patterns (Auzende et al., 1973; Galdeano and Rossignol, 1977). The magnetic fabric which is best expressed in the Western Mediterranean is found in the EAB where a NW-SE fan of alternating positive and negative lineations was first described by (Bayer et al., 1973) and is limited to the east by the North Balearic Fault Zone forming the so-called Hamilcar magnetic anomaly (Mauffret et al., 2004).

2.2 Summary of previous kinematic reconstructions

We review here the main kinematic reconstructions proposed for the Miocene rifting and seafloor spreading of the AB basin. Models appear to differ significantly owing to the lack of constraints on the age of the magnetic anomalies and of deep drillings reaching the basement. It is worth noting that in most published models, the Alboran domain was either not taken into account or placed at different positions without clear space and time kinematic constraints. Conversely, all models agree with a NW-SE early opening of the Liguro-Provençal basin starting ca. 23 Myr ago, with a well constrained counterclockwise rotation of the Corsica-Sardinia block assumed to be in its present day position at 16-15 Ma (Gattacceca et al., 2007; Speranza et al., 2002).

Each proposed model inherently comes with its own assumptions, simplifications and omissions, and therefore strongly differs from the others regarding the timing and chronology of opening of the AB sub-basins and the position of the retreating subduction. These models can be classified into two major types with contrasting timing, i.e. one-step or two-step models: 1- one-step opening by progressive SE-directed rollback of the Tethyan slab (Schettino and Turco, 2006); modified from previous simplified scenario such as the ones by (Gelabert et al., 2002; Gueguen et al., 1998; Jolivet and Faccenna, 2000), as well as the double-saloon door opening proposed by (Martin, 2006); 2- Diachronous opening model during Miocene times proposed by (Cohen, 1980; Driussi et al., 2015; Mauffret et al., 2004; van Hinsbergen et al., 2014).

In order to further describe the peculiarities of existing models, we have redrawn on Figure 2 the four types of kinematic models proposed until now to explain the birth and opening of the AB basin. They favor either N-S (Figure 2a,b) or E-W (Figure 2c) dominant directions of opening and sometimes combine successively both directions during Miocene times (Figure 2d).

a) Model 2a of Schettino and Turco (2006) is based on a new interpretation of magnetic anomalies and balanced crustal cross sections, leading to assume an early opening of the whole AB basin (mainly during the 30-19 Ma time span) coeval to the southward migration of the Kabylies and to the rotation of Corsica-Sardinia block, i.e. synchronous to the opening of the LP basin. This model involves a complex spreading system with R-R-R triple junctions and eleven microplates but does not include the Alboran plate (Figure 2 a).
b) Model 2b of Martin (2006) is a more conceptual model based on the hypothesis of a "double-saloon-door" opening. A synchronous opening of the Algerian basin (eastern and western one) and the Liguro-Provençal Basin is also assumed as a consequence of two opposite rifts allowing the saloon door opening of a third basin in between, representing the AB basin. A bilateral propagation of Tethyan slab detachments is assumed to trigger this opening mechanism, but time constraints on seafloor spreading (assumed to range between 19 and 15 Ma) are lacking.
c) Model 2c of Mauffret et al. (2004) suggests a late opening of the Algerian basin along a NW–SE spreading center between 16 and 8 Ma, i.e. after the collision of the Kabylian terranes with the African margin and the rotation of the Corsica-Sardinia block. According to this model, the Alboran domain was close to the EAB and then moved about ca. 630 km westward along transform zones located north and south of the Algerian margin after 16 Ma.
d) Model 2d (Cohen, 1980; Driussi et al., 2015) is based on interpretations of the position of slab segments from seismic tomography. It assumes that the oceanic accretion of the EAB occurred together with the southwestward drift of LK between 19 and 16 Ma.

This review shows that except the model of Mauffret et al. (2004), all published kinematic models consider that the opening of the East Algerian basin, the drift and docking of the Kabylian blocks and the last phase of the Corsica-Sardinia block rotation occur during the same time period. Furthermore, they all assume an opening of the EAB prior to 15 Ma (except again model c), i.e. more or less during the opening of the LP domain (Figure 2).

The two-step kinematic scenarios (Figure 2c, d) are assuming that at least the opening of the western and central AB basin occurred after the south-south-westward drift of Kabylian terranes. Although they provide different ages for the EAB, they agree with a STEP (Subduction-Transform-Edge-Propagator) fault evolution of the Algerian margin characterized by a significant westward motion of the Alboran block and a bilateral Tethyan slab tearing or fragmentation responsible for backward migration of narrow slabs and formation of the narrow and tight Calabrian and Gibraltar arcs (Chertova et al., 2014; Faccenna et al., 2004; van Hinsbergen et al., 2020, 2014). However, model c lacks compelling evidence of stratigraphic and paleomagnetic records and model d clearly contradicts field and offshore evidence showing that the LK continental margin was stretched in a NW-SE direction (Arab et al., 2016b, 2016a; Bouillin, 1986, 1977). In contrast to previous assessed reconstructions, we attempt to build an updated kinematic model of the AB basin by addressing the history of the Eastern Algerian Basin (EAB) as well as the tectonic history of the Alboran domain.

2.3 Sedimentological and stratigraphic record of the Eastern Algerian continental margin

Northern Algeria is part of the Alpine orogenic system resulting from the collision of AlKaPeCa terranes with the North African margin. In our study area, it is referred to as the Maghrebide belt (Figure 1) (Durand Delga, 1980; Frizon de Lamotte et al., 2004). The onshore domain is divided into inner and outer zones and composed of several well-described geological

formations outcropping in LK and GK blocks and further south (Bouillin, 1977; Bouillin and Raoult, 1971; Vila, 1980). The inner zones ("Kabylide domains") are made of crystalline (as part of the AlKaPeCa blocks), sedimentary and magmatic formations , while the Tellian nappes represent the external zones. These two domains are separated by a suture zone and covered by flysch units of various ages. We focus here on the Oligo-Miocene sedimentary formations that were deposited on land in order to correlate them with their analogue offshore units interpreted from the seismic sections. For this reason, we rely on a detailed analysis of sedimentary outcrops in terms of depositional environments, sedimentary structures and biological contents of several sub-basins of Lesser Kabylia carried out by Arab et al. (2016b) (Figure 3). These onland sedimentary deposits of the Eastern Algerian margin represent the proximal continuation of the marine deposits found in the EAB which were connected before the emersion of the margin during Middle to Late Tortonian times (Arab et al., 2016a, 2016b; Carbonnel and Courme-Rault, 1997).
In Lesser Kabylia, only the Langhian formations have been preserved on land, while in the external zones, Late Burdigalian-Langhian to Tortonian units rest on top of the flysch deposits of the Tellian allochthon (Arab et al., 2016b; Bouillin, 1986; Carbonnel and Courme-Rault, 1997). After basin-scale correlations from land to sea, the following pre-Messinian units have been identified (Figure 3):

(1) PMU1: The chaotic facies and hummocky structure of Unit 1 (PMU1) is correlated to the conglomeratic clastics of the Oligo-Miocene Kabyle 'OMK' formation (dated Aquitanian-Burdigalian) of LK and GK. It is formed by a fining upwards conglomerate overlain by lenticular sandstones to sandy blue marls and limestones dated at 19 ± 1 Ma (Aïte and Gélard, 1997). It characterizes a littoral environment and a transgressive sequence interpreted as a syn-rift deposit at the opening of the backarc basin, deformed with the Kabylian basement during and after the collision of the Kabylian block with Africa. The transgressive trend was dominant from the Upper Burdigalian to the Langhian according to global eustatic charts from (Haq and Schutter, 2008). The Numidian flysch nappes were emplaced by gravity sliding over the OMK unit (Aïte and Gélard, 1997).
(2) PMU2: This first post-rift sequence begins with breccia and conglomerates followed by thick layers of sandstones and blue marls of Langhian age. These Langhian units depict a transgressive trend with lateral variations related to tectonic, sedimentary or eustatic controls. This unit is characterized offshore by a parallel configuration of reflectors which indicates a uniform sedimentation in a deeper marine environment beyond shelf break. Onlaps at the margin toe evidence the Langhian transgression defined on outcrops, while hummocky facies is interpreted as turbidite deposition.
(3) PMU3: On land, the second post-rift unit is dated from the Serravallian and consists of grey marls overlain by conglomerates and argillaceous sandstones. The described facies indicate an evolution toward continental environments and a regressive trend. Based on the facies models from Veeken (2007), the chaotic features at the top of this unit offshore indicate an overpressured shale that can be correlated to the blue marls observed in the field, while the high frequency content of reflectors may indicate facies dominated by fine-grained sediments.
(4) PMU4: The last pre-Messinian unit onshore is dated from Tortonian and consists of grey sandy shales with gypsum and oysters at its base, evolving to conglomerates intercalated with blue-grey shales and reddish continental sandstones at the top. This regressive trend indicates a gradual relative uplift of the margin. Due to the pull-up effect of salt and

velocity inversion (e.g., Jackson and Hudec, 2017), this unit forms a poorly reflective subsalt zone on the seismic lines, preventing us from correlating it with the onland unit.

The Tortonian sequence is topped by a major unconformity onshore, ascribed to the Messinian Main Erosional Surface (MES) and probably linked to first indices of tectonic inversion of the Algerian margin (Arab et al., 2016b; Recanati et al., 2019). Therefore, Messinian series were most probably not deposited in the onshore part of the study area. In the Western Algerian basin, a unit consisting of plastic gray marls and gypsum is interpreted as the lower unit of the Messinian sequence (Medaouri et al., 2014). Off Bejaia and Skikda, the Lower Messinian Unit (LU) shows lateral seismic facies changes with chaotic facies revealing a high-energy environment and detritical deposition before salt precipitation, as found elsewhere in the Mediterranean sea (Granado et al., 2016; Lofi et al., 2011).

In the following, these lithologies and eustatic trends are associated with specific facies and angular unconformities interpreted on seismic sections. The recent tectonic inversion has also deformed the upper slope of the margin, therefore a detailed reconstruction of paleobathymetry, paleomorphology and paleogeography from seismic data is beyond the scope of this study.

3 Data Set and methods

Our study zone spans the Eastern Algerian offshore covering the well identified magnetic anomalies zone which extends from Bejaia to Annaba cities with an area of about 62.103 km2. Due to the lack of available well data, absolute ages and lithologies are unconstrained for the seismic units in the deep Algerian basin. Accordingly, we integrated a large set of geophysical and geological data such as multichannel seismic data (MCS), wide-angle seismic profiles, vintage academic profiles and reduced-to-the pole magnetic anomalies. In order to compensate to some extent the lack of absolute ages, we based our study on a seismo-stratigraphic age model extrapolated from onland sedimentary strata correlated with offshore analogue sedimentary units as reported by Arab et al. (2016b).

3.1 Seismic data

For this study, we use mainly a set of deep penetrating seismic reflection lines (10 s TWT) designed to image the sedimentary units below the widespread Messinian salt including crust and Moho reflectors. These 2D multi-channel sections labelled "L" (Figure 4) have been recorded in the Algerian offshore by WesternGeco in 2000-2002 (Cope, 2003) using a sleeve tuned air gun array (3000 inch3) as a seismic source towed at 6 m depth. The shot points were spaced by 25 m, the processing sample interval is 4 ms and the processing record length is 10,000 ms. Among this database, two E-W profiles (L5 and L6) in the main depot-center of Bejaia canyon have been used to describe in detail the pre-Messinian sedimentary infill that recorded key information to understand the basin sedimentary evolution (Figure 4). Additionally, nine seismic profiles from the SPIRAL cruise were used and labelled “SPI” (Figure 4), among them two wide-angle seismic profiles (SPI14 and SPI22) have been used to locate the continent-ocean transition (Bouyahiaoui et al., 2015; Mihoubi et al., 2014) in our study region. MCS Line SPI18 is coincident with the wide-angle seismic profile SPI22. The SPIRAL multichannel seismic data set was acquired in 2009 aboard the R/V L’Atalante using a 4.5-km-long streamer composed of 360 channels spaced at 12.5 m interval enabling the acquisition of deep frequency 2D MCS profiles. The seismic source consisted in an air-gun array of various volumes (3040-8909 inch3), with 50-150 m shot spacing

(Graindorge et al., 2009). Owing to the low frequency (~25 Hz), the resulting seismic sections have a deep penetration able to image the deepest crustal structures down to the Moho. Besides "SPI" and "L" profiles, we also used a set of vintage seismic profiles labelled "ALE". These seismic lines were acquired by Total in the 1970s (Mauffret, 2007), and consist of high-resolution, scanned and georeferenced images of paper-copies that were digitized into SEGY format. In addition, a set of OGS (National Institute of Oceanography and Applied Geophysics) seismic lines labelled "MS" were used to ensure the coverage of the northern and eastern part of our triangular zone. They were acquired by OGS aboard the R/V Marsili between 1972 and 1979s, using a 2.4km-long and 10m-depth streamer, with a sample rate of 4 ms. The seismic source consisted of 3 guns and microcharges of 50 g (Geodin - B), with 50-100 m shot interval and a dominant frequency of 100 Hz (Finetti and Morelli, 1972). All seismic profiles were loaded onto IHS Kingdom software in order to benefit from a single, consistent interpretation project.

Our adopted methodology is based on the detailed seismostratigraphic interpretation of seismic units, their stratal terminations and configurations including onlaps, toplaps, downlaps and their bounding surfaces interpreted as chronostratigraphic time lines using seismic stratigraphic concepts (Veeken, 2007). The parameters in seismic facies analysis taken into consideration are reflection amplitude, dominant reflection frequency, reflection continuity and configuration, geometry of seismic facies, and relationship with other units. Arab et al. (2016b) used both direct and indirect interpretations in order to predict the lithology corresponding to the seismic facies unit and to highlight depositional environments and sedimentary cycles (transgression, regression, erosion). In order to tie and adjust seismic interpretations and to check the consistency of facies distribution and lateral changes, eighty-two crossing points between multi-scale resolution seismic lines were analysed. The results of the seismic facies analysis is shown on seismic facies cross-sections and the seismostratigraphic units are correlated by their corresponding age following the age model (Figure 5). The seismic data are presented in two-way-time (TWT) and the unit velocities are taken from Arab et al. (2016a).

Using the interpreted key horizons (R5 & B) (Figure 4) exported from the IHS Kingdom software, we created two surfaces using the © Petrel software. These horizons were selected based on their significance in relation with the major geodynamic event of the opening of the Eastern Algerian basin. We also compiled various existing basement grids off Sardinia and the Balearic Islands from Driussi et al. (2015) and Leroux et al. (2019) in order to build a detailed new map with a uniform geographic coordinate system covering the entire Eastern Algerian basin. A 500 m grid cell from the TWT values of the surfaces were modelled using the minimum curvature gridding algorithm that allows us to perform seismic-based time-structure maps for the acoustic top basement and pre-salt sequence. These illustrate respectively the depth and lateral thickness changes within the Eastern Algerian basin.

3.2 Magnetic data

The first almost complete, high-resolution magnetic anomaly map covering the entire western Mediterranean basin was built thanks to several aeromagnetic surveys led at a constant height of 600 m and carried out between 1966 and 1974 (Galdeano and Rossignol, 1977). The resulting map shows well-defined magnetic lineations in the South-West of Sardinia resembling those first described by (Vine and Matthews, 1963) and relating to the opening of the EAB (Bayer et al., 1973; Cohen, 1980; Galdeano and Rossignol, 1977). Later on, different researchers (Driussi

et al., 2015; Schettino and Turco, 2006) have reproduced other versions of this map and proposed several interpretations, however these compilations do not provide more detailed features in the EAB. In order to improve the interpretation of the magnetic anomalies, we have used a reduced-to-the-pole (RTP) magnetic anomaly (MA) map (Figure 6a) that provides fundamental constraints on the mode and timing of oceanic spreading. The magnetic data used in this study were recorded in 1977 by the American geophysical company Tidelands with a flight line mesh of 15x10 km covering the Algerian basin. These were 1:100,000 scale maps representing raw magnetic anomalies with an iso-line interval of 10 nT. The data were digitized and filtered to obtain and then used for the raw data pole reduction (Medaouri et al., 2014). The resulting magnetic map shows a good correlation and coincidence with the major regional patterns found in existing maps of the Western Mediterranean, including the Algerian basin (Auzende et al., 1973; Bayer et al., 1973; Galdeano and Rossignol, 1977; Schettino and Turco, 2006).

3.3 Construction of the age model

Unfortunately, the only deep well drilled in the eastern Algerian offshore (DSDP site 371) is located at about 102 km from the shoreline in the deep basin off Bejaia, with 551 m of sedimentary cover at 2792 m water depth and only 5 m of Messinian upper unit were reached (Hsu et al., 1978). Consequently, we were not able to perform a well-to-seismic calibration, nor to use it as a surface analogue for the offshore pre-Messinian series and to go further in seismo-stratigraphic interpretation of the seismic profiles. Therefore, we follow here a conventional approach to (1) compute relative ages of the first pre-Messinian units overlying the oceanic crust based on their thicknesses and (2) predict mean age and seafloor spreading rate of the EAB. Note that we focus primarily on the relative age of units based on seismo-stratigraphic analysis, rather than the absolute ages. The methodology is based on time-to-depth conversion (sTWT to m) of sedimentary thicknesses using interval velocities of the first pre-Messinian units deposited on the oceanic crust (PMU2 and PMU3). The Petrel software was used to generate interval velocities between picked horizons using stacking velocities and the Dix formula (Dix, 1955) (Figure 5).

The seismo-stratigraphic interpretation is based on a seaward prolongation of the four pre-Messinian units (PMU1 to PMU4) identified in the stretched continental margin of Lesser Kabylia by Arab et al. (2016b) (Figure 5). It has allowed us to divide the EAB into two parts according to the first pre-Messinian unit deposited on the oceanic crust. The first one is identified above the N2e, R2w, N1e and R1 magnetic anomalies, where the PMU3 unit (Serravallian) is directly deposited on the oceanic crust. The second one is found above the R4w, N3w and R3w magnetic anomalies where PMU2 (Langhian) is the first unit deposited. We rely on the age model of Arab et al. (2016b) to date the PMU3 and PMU2 units which are assumed to represent respectively the Serravallian and Langhian time spans. Using the thickness (converted into meters) of the pre-Messinian units interpreted from the seismic lines, we consider as a starting point that at N2w anomaly, the first unit PMU3 overlying the oceanic crust is deposited in the entire Serravallian, and that R2 and R3 reflectors mark the transitions from Langhian to Serravallian times (13.82 Ma) and from Serravallian to Tortonian times (11.63 Ma) respectively (Cohen et al., 2013). By assuming that the sedimentation rate was constant during the Serravallian, we then compute the relative ages of the parts of Unit PMU3 deposited above magnetic anomalies R2w, N1w and R1 based on their different thicknesses. From this calculation, we obtain a time interval corresponding to the opening of the first part of the EAB and to the sedimentation time interval for PMU3 deposition. This allowed us to calculate the seafloor spreading rate and the sedimentation rate for

this part of the basin where only the Serravallian units of different thickness cover the oceanic crust. We follow the same calculation approach to compute the relative ages of PMU2 units deposited on the oceanic crust for the second, oldest part of the EAB, where PMU2 is the first unit deposited. Since we do not know whether the PMU2 unit above R4w magnetic anomaly covers the entire Langhian time or only part of it, we first assume that the seafloor spreading rate remained constant during Serravallian and Langhian times (Hypothesis A). Based on this first assumption, we compute the relative ages for the PMU2 units deposited above R4w, N3w, R3w anomalies based on their respective thicknesses. We obtain the time interval during which the second part of the EAB is opened and also the sedimentation time and rate for the PMU2 unit. Finally, in order to bracket age uncertainties, we perform a new calculation considering a second assumption, i.e. that the sedimentation rate during Langhian and Serravallian time was constant, leaving seafloor spreading rate unfixed (Hypothesis B). This allows us to compute new relative ages of PMU2 and PMU3 units as discussed above. The lower part of Table 1 summarizes the mean values of ages, accretion time and half-spreading and sedimentation rates with their standard deviation (SD) by including all hypotheses (A and B).

A) Ages and associated SD (Ma) assuming **a steady seafloor spreading rate** and **variable sedimentation rates** in Langhian and Serravallian times	**Langhian** (15.97 - 13.82 Ma)			**Serravallian** (13.82 – 11.63 Ma)			
	Sedimentation rate: 627.7 +/- 11			Sedimentation rate: 482.5 +/- 0.3			
	T7	T6	T5	T4	T3	T2	T1
	U2 (R4w)	U2 (N3w)	U2 (R3w)	U3 (N2w)	U3 (R2w)	U3 (N1w)	U3 (R1w)
	15.01 ± 0.02	14.65 ± 0.01	14.54 ± 0.01	13.82 (fixed)	13.49 ± 0.03	12.97 ± 0.02	12.74 ± 0.02
	Accretion time span (Myr): 2.27 ± 0.04						
	Steady half-spreading rate (mm/yr): 41.5 ± 0.7						
B) Ages and associated SD (Ma) assuming **a steady sedimentation rate** and **variable (unfixed) seafloor spreading rates** in Langhian and Serravallian times	**Steady sedimentation rate (m/Ma):** 482.5 ± 0.3						
	T7	T6	T5	T4	T3	T2	T1
	U2 (R4w)	(N3w)	U2 (R3w)	U3 (N2w)	U3 (R2w)	U3 (N1w)	U3 (R1w)
	15.37 ± 0.01	14.91 ± 0.01	14.75 ± 0.01	13.82	13.49 ± 0.03	12.97 ± 0.02	12.74 ± 0.02
	Accretion time span (Myr): 2.63 ± 0.02						
	Half-spreading rate: 31.9 ± 0.1			**Half-spreading rate:** 41.5 ± 0.7			

Final values and uncertainties considering all hypotheses (A and B)							
Mean ages and associated SD (Ma)	15.19 ± 0.18	14.78 ± 0.12	14.64 ± 0.11	13.82	13.49 ± 0.03	12.97 ± 0.02	12.74 ± 0.02
Mean accretion time span (Myr) : 2.45 ± 0.18 Mean seafloor half-spreading rate (mm/yr) : 36.7 ± 4.8 Mean sedimentation rate (m/Ma): 555.1 ± 72.6							

Table 1. Mean predicted ages and half-spreading rates of the EAB midway from the rotation pole (see Figure 6). Values and standard deviations are computed after time-depth conversion using mean interval sonic velocities (Figure 5). T1-T7 = isochron ages obtained from depth conversion (see text for details). T4 = fixed age (13.82 Ma) between Langhian and Serravalian times (Cohen et al., 2013). SD = Standard Deviations computed using the hypotheses A and B (left-hand column). The lower part of the Table brackets the values of ages, accretion time and half-spreading rate by considering hypotheses A or B. The terms slow, intermediate, fast, and superfast spreading refer to full spreading rates of <40 km/Myr, 40–90 km/Myr, 90–140 km/Myr and >140 km/Myr, respectively.

It is important to note that a "true" estimation of the calculated ages and rates is difficult to obtain due to various sources of uncertainties, especially those related to the assumptions on the age model and to the limits of seismic correlations between sections shot with different sources and processed independently. Other sources of errors come from (1) the vertical resolution of picking, depending on the seismic resolution, (2) uncertainties on seismic velocities (few hundred m/s) and consequently the time-depth conversion, and (3) inaccuracies in the available lithologies and their lateral variations. Furthemore, we were not able to check the robustness of our calculations on the western part of our triangular zone due to the lack of data and its low resolution. Owing to these limitations, we have no way to improve the true estimates on these parameters, so we propose to consider the final uncertainties on ages and rates after using both hypotheses A and B as a first approximation of "true" values and as a test of consistency to our kinematic model, to be compared with other models of accretion and sedimentation in similar geodynamic contexts.

4 Results

4.1 Analysis of magnetic anomalies

Based on previous interpretations of RTP-MA maps of the AB (Bayer et al., 1973; Medaouri, 2014; Medaouri et al., 2014; Driussi et al., 2015; Aïdi et al., 2018), we have performed a new analysis that allows us to identify 3 regions in the deep basin with different magnetic patterns: (1) NO – SE fan-shaped pattern, (2) Hannibal high, (3) and a "fragmented" pattern.

The magnetic pattern (1) is striking N-S and NW-SE along the western and eastern edges of the EAB between 5°E - 9°E (Figure 6). The fan is ~320 km wide along the continental margin and ~210 km long from the rotation pole located near 39°02'N and 5°18'E (Cohen, 1980). It is approximately bounded by the 2500 m isobath and is nicely expressed over the whole Eastern

Algerian basin (Driussi et al., 2015; Galdeano and Rossignol, 1977; Schettino and Turco, 2006) and their amplitudes reach a peak of 250 nT (Figure 6a) . This pattern of magnetic anomalies likely evidences the formation of oceanic-type crust around a close rotation pole and is geometrically related to the westward motion of the Alboran domain assumed by many authors to be driven by the Tethyan slab tear toward Gibraltar (e.g., (Chertova et al., 2014; D'Acremont et al., 2020; Do Couto et al., 2016; Romagny et al., 2020; van Hinsbergen et al., 2014). We use the geometry of the fan-shaped magnetic anomaly zone (RTP-MA map, Figure 6) to fit several hypotheses on the symmetry of accretion according to normal and reverse polarities. Our best adjustment suggests 13 roughly symmetrical magnetic anomalies striking NW-SE and pointing to a close rotation pole east of the Balearic block (Figure 6b). Six magnetic polarity reversals are symmetrically distributed besides a central accretion of negative polarity of a few hundred nanoTesla (350 nT). We assume that the westernmost negative anomaly (R4W) has been partly disturbed by late volcanic activity near the Hannibal High (Aïdi et al., 2018; Mauffret et al., 2004). However, some polarity reversals have so short durations during Miocene times (Gee and Kent, 2007; Gradstein et al., 2012) that they could be missed in our analysis of seafloor anomalies. Whatever the case, the contrasting pattern of magnetic anomalies in the Western Algerian basin (WAB) suggests a major change in the way back-arc opening worked after the emplacement of the EAB oceanic basement.

Between 4°E - 5°30'E, the Hannibal magnetic anomaly (2) is characterised by a sub-circular group of high amplitude positive magnetic anomalies about 250 nT and 70 km wide. It is understood as a cluster of basement highs built by stacking of Miocene volcanic and volcaniclastic bodies over a thin oceanic crust, representing possibly an offshore equivalent of the post-collisional calc-alkaline magmatism of Lesser Kakylia (Chazot et al., 2017) but with a clear Miocene post-accretion activity (Aïdi et al., 2018; Mauffret et al., 2004).

In the central and western parts of the Algerian basin, fragmented magnetic anomalies pattern (3) have been interpreted as the result of irregular and sporadic accretion processes at the rear of the subduction zone (Medaouri et al., 2014). Between Ténès and Tigzirt, three NW-SE alignments of high amplitude (150 and 250 nT) trend obliquely to the margin. The anomalies located between 0°E and 3°E show a high amplitude reaching 250 nT (Figure 6a) and could correspond to magmatic bodies. These anomalies would locate potential extinct seafloor spreading centers (SC) offset by NE-SW trending oceanic transform faults (OT1, OT2) (Medaouri et al., 2014). They are limited southward by a linear stripe of magnetic low featuring the outward limit of the STEP1-fault (Leprêtre et al, 2013; Medaouri et al., 2014). Further west, between Ténès and Oran, the magnetic structure reveal a large, high amplitude anomaly in the center and again a linear stripe of magnetic low at the margin toe that could mark the outward limit of the STEP2- fault (Badji et al, 2014; Medaouri et al., 2014). Finally, the large (50-70 km wide) stripe of relatively high magnetic anomalies between STEP 1-2 faults and the coastline with variable amplitude and direction would sign thinned continental fragments accreted to the margin (Medaouri et al., 2014).

4.2 Seismo-stratigraphic interpretation

Based on our interpretation on regional 2D seismic sections, we subdivide the sedimentary cover of the Eastern Algerian margin and basin into three major stratigraphic sequences from bottom to top as follows: pre-Messinian, Messinian and Plio-Quaternary. Each sequence is subdivided into several units and has its own stratigraphic characteristics. Each unit is separated

from the other ones above and below by a horizon-reflector interpreted as a chronostratigraphic time line of which nine horizons have been identified, including the basement top and seafloor (Figures 5 and 6). As discussed in Part 2.3 above, the interpretation of each identified Pre-Messinian seismic facies is based on (and in good agreement with) the stratigraphic and sedimentological correlations between the onshore and offshore formations performed by Arab et al. (2016b). The Messinian and Plio-Quaternary units are consistent with stratigraphic models already proposed for the Mediterranean basin (e.g., Granado et al., 2016; Lofi et al., 2011) and are not discussed here, since they appear to post-date the formation of the BA basin (Camerlenghi et al., 2008; Dal Cin et al., 2016).

Figure 7 (a to f) illustrates several intersections of crossed seismic lines or a single profile extractions interpreted from our database (Figure 4). These seismic extractions emphasize the lateral consistency of facies distribution, characterize the major variations in the depth of seismic horizons and display the changes of the thickness of pre-Messinian units. Despite the diversity of the seismic images in terms of resolution and penetration, we have selected the most accurate and robust correlations from eighty-two crossing points between multi-scale resolution seismic lines. Accordingly, four pre-Messinian units, referred to as PMU1 (oldest) to PMU4 (youngest), have been identified (Figure 5-7). These units are separated from the acoustic basement and from each other by eight horizons interpreted as chronostratigraphic lines. These are from bottom to top as follows: B, R2 to R8. The deepest horizon represents the top of the acoustic basement that separates the crust from the overlying Neogene sedimentary units. It is clearly identified as a strong high amplitude reflector on all analyzed seismic lines of good penetration. The main characteristics of pre-Messinian seismic units and their limits/horizons are briefly described below.

The synrift deposit on the continental crust is referred to as the Pre-Messinian Unit 1 (PMU1) (Figure 5). In the Bejaia Gulf, Jijel and Annaba area, PMU1 is a high-amplitude, moderate frequency, and high impedance seismic package separated from the underlying basement. It generally displays a hummocky configuration with discontinuous reflectors. Although, the facies of PMU1 shows lateral change, depicting continuous sub-parallel reflectors or chaotic facies as well as a vertical change (Arab et al., 2016a, 2016b). On seismic profiles L1 (N-S) and L5 (E-W), the PMU1 shows clear onlaps configuration on a basement high or half grabens (Figure 5). Along the offshore Eastern Algerian margin, PMU1 deposits only on the continental crust where it pinches out before reaching the oceanic crust. It is deformed and faulted (L3, L5 profiles), marking the syn-rift period in the Eastern Algerian deep basin (Arab et al., 2016b).

The first post-rift unit is referred to as the Pre-Messinian Unit 2 (PMU2) (Figure 5). In the stretched continental margin, it is separated from the underlying unit by the B horizon that represents an unconformity between PMU1 and PMU2, making the transition from Aquitanian-Burdigalian to Langhian times. The PMU2 is a high to moderate amplitude, low to moderate frequency seismic package characterized by sub-continuous sub-parallel reflectors with onlaps and limited to the top by R2 representing an unconformity marked by toplaps (Figure 7 a,b). In some parts, the PMU2 facies is disturbed by salt pull-up effects and evolved to chaotic facies in the deep basin (e.g., L3). On the L5 section (Figure 5), PMU2 depicts onlapping reflectors against the PMU1 and the basement high. East of Cape Bougaroun (L3-L8 and others SPI and ALE sections), PMU2 is deposited only over the continental crust, marking the transition from N2 to R2 anomalies.

In the Bejaia area, the second post-rift unit PMU3 displays a set of sub-parallel reflectors of high amplitude and moderate frequency (Figure 5) evolving to chaotic facies with discontinuous reflectors within the deep basin (Figure 7 b). In the Jijel area and off Cape Bougaroun, PMU3 consists of a seismic package of low to moderate amplitude, intermediate frequency and sub-continuous reflectors (Figure 7c, L2, L3, L4 profiles). It evolves towards chaotic facies in the deep basin (e.g., L3 section) and towards sub-horizontal reflectors with low amplitude, moderate frequency off Annaba (Figure 7 e,f). It is separated from PMU2 and PMU4 units by downlaps on R2 (Figure 7 b) and by toplaps and downlaps on R3, respectively (Figure 7 b,c,d, f).

The last post-rift unit (PMU4) is defined off Bejaia by parallel to wavy reflectors of high amplitude and moderate to high frequency (Figure 5). In the deeper basin, it changes to parallel and sub-horizontal reflectors of low to moderate amplitude and frequency (Figure 7a,b) and exhibits apparently chaotic facies on some areas due to pull-up effects. Off Jijel, it forms a low to moderate amplitude and moderate frequency seismic package with sub-parallel reflectors in the deeper area and shingled facies on the proximal area, passing laterally to chaotic facies (L2 profile). Off Cape Bougaroun, PMU4 displays a shingled facies of high amplitude and high frequency seismic package passing laterally to chaotic facies with discontinuous reflectors of moderate amplitude in the deep basin (Figure 7 c,d). Off Annaba, it displays a set of subparallel reflectors with low amplitude and moderate frequency, laterally passing to chaotic facies (Figure 7 e,f). PMU4 is separated from the PMU3 and LU units by downlaps on R3 (Figure 7 c) and by toplaps and downlaps on R4 (conformable in the deep basin, locally erosive at the margin toe), respectively (Figure 7 c,d,f).

All three post-rift units show clear onlaps over the PMU1 unit (Figure 5). The facies interpretation of the PMU1-2-3-4 is in good agreement with the stratigraphic and sedimentological correlations between the onshore and offshore formations (Arab et al., 2016b) (Figure 3).

4.3 Isopach mapping

Our seismic interpretation allows us to generate isopach maps helping to account for the absence of deep wells reaching the pre-Messinian sequence in the northernmost part of the EAB. These maps display the variations of the depth of the acoustic basement (Figure 8 a) and the thickness of the seismic pre-salt sequence (Figure 8 b) in seconds TWT. The top basement (B) map clearly evidences a large (i.e. 80-120 km wide) topographic high striking NW-SE pointing toward the paleomagnetic pole and displaying a symmetrical, gentle deepening on both sides (Figure 8 a), a pattern which clearly recalls the morphology of oceanic ridges. The centre of this topography is at ca. 1.2 s TWT above the deepest parts of the basin (from 5.2 to 6.4 s TWT depth, respectively) and coincides fairly well with the R1 magnetic anomaly. Similarly, the pre-Messinian isopach map reveals a clear trend from the edges of the basin toward its center, with an estimated maximum thickness of about 1.2 sTWT in the westernmost R4W magnetic anomaly (Figure 8 b). The thickness decreases to less than 0.15 s TWT in the center of the basin above the R1 anomaly. The across-axis relief from R1 to R4 magnetic anomalies is of about 2 km for a mean velocity of 3.5 km/s (Figure 5). Besides, the thickness of the pre-Messinian sequence decreases northward as well as towards the upper slope of the margin, where only the Messinian erosional surface (MES) remains. Note that the deepest area of the basin is found facing Cape Bougaroun, about 30 km from the shoreline: this sub-basin has recorded the most complete Neogene and Quaternary sedimentary history (Arab et al., 2016a, 2016b).

These maps also show that the southern EAB is structured by several basement highs (profiles SPI13, L1, L5, L6, L7 and SPI18, Figure 4b). These basement highs often coincide with magnetic anomalies and are interpreted as volcanic massifs outcropping at Cape Bougaroun, Cap de Fer and Cape El-Ouana in the continental margin (Figure 4a) (Arab et al., 2016b) or above the oceanic crust (Arab et al., 2016b; Bouyahiaoui et al., 2015). They are assumed to result from the Tethyan slab break-off, similarly to the Collo massif on land (Abbassene et al., 2016; Chazot et al., 2017).

4.4 Stratigraphic relative age model

Our seismo-stratigraphic interpretation shows that the first unit deposited on the oceanic crust at N2w anomaly away from the central anomaly by 44.6 km, is the PMU3 unit between reflectors R2 and R3. Accordingly, based on the age model of Arab et al. (2016b), we assume that this 510 m thick unit (for a mean velocity of 3520 m/s) was deposited during the entire Serravallian period of 2.19 Ma, considering that the R2 reflector marks the transition from Langhian to Serravallian times at 13.82 Ma and that the R3 reflector marks the transition from Serravallian to Tortonian times at 11.63 Ma (Cohen et al., 2013). Assuming a constant sedimentation rate during the Serravallian, we calculated the relative ages for the other PMU3 units deposited above R2w, N1w and R1 magnetic anomalies from their respective thicknesses (440, 316.8 and 264 m). Therefore, we obtain from this calculation a time interval of 1.06 Ma corresponding to the spreading duration for the first part of our basin (R1, N1w, R2w and N2w magnetic anomalies, Figure 6) and consequently to the deposition of the PMU3 unit. From this time interval, we were able to calculate a seafloor spreading rate of 42.2 mm/yr and a sedimentation rate of 482.7 m/Ma for this basin part where only the Serravallian units overlie the oceanic crust. To calculate the relative ages of the PMU2 unit deposited directly on the oceanic crust in the second part of our basin along R4w N3w, R3w and as we were unable to ascertain if the PMU2 unit at R4w anomaly was deposited in the entire Langhian times, we assumed that the seafloor spreading rate remained constant during Serravallian and Langhian times (Hypothesis A). Based on this assumption, we follow the same calculation procedure. Although the PMU2 unit at R4w is of 748 m (for a mean velocity of 3740 m/s) and about 50 km away from the central anomaly. Therefore, the relative ages for the other PMU2 units deposited above N3w and R3w is calculated from from their respective thicknesses (523,6 448,8m). The resulting theoretical spreading time span is about 1.17 Ma necessary to the sedimentation of the PMU2 unit along the R4w N3w and R3w anomalies with a sedimentation rate of 627 m/Ma.

Additionally, we use a second assumption (Table 1, Hypothesis B) with steady sedimentation rate in Langhian and Serravalian times in order to improve the estimation of age uncertainties and to test the consistency of our analysis. By considering successively hypotheses (A and B) and propagating all the sources of errors, our results reveal that the seafloor spreading of EAB occurred with an intermediate to fast half-spreading rate of 3.7±0.5 cm/yr during 2.45±0.18 Myr between 15.19 ± 0.18 Ma (Langhian) and 12.74 ± 0.02 Ma (Serravallian).

5 Discussion

5.1 Chrono-lithostratigraphic evolution of the Eastern Algerian basin

We present here a seismostratigraphic synthesis showing the evolution of the East Algerian basin along an E-W transect cutting the western and eastern part of our triangular area as shown in the inset (Figure 9). We have successfully followed the thickness and depth of the pre-Messinian units, as well as the depth of the top of the basement along our basin and consequently obtain a comprehensive, synthetic view of the evolution of the basin. It was performed from the crossing points between the seismic profiles as well as from individual seismic sections. Each point labeled from A to G on the western side, then from G to A' on the eastern one is located over a magnetic anomaly strip from R4W to R4E respectively (Figure 6). Although we were not able to clearly identify all seismic units on some seismic sections, we succeeded in comparing the depth of the top of the basement and the base of the salt and therefore the thickness of the pre-Messenian sequence. Note that according to our land-sea correlation of seismic facies and sedimentary outcrops, the oldest units overlying the oceanic floor are of Langhian age (15.97 – 13.82 Ma), i.e. younger than the syn-rift deposits identified on the stretched continental crust of Lesser Kabylia (Arab et al., 2016b). Due to the quality of the seismic profiles in the eastern side of the triangular zone, we have relied on the Ms profiles (Figure 4b) to compare the stratigraphic evolution of the basin by comparing the thickness of the pre-salt sequence on the both western- eastern sides. Our results show that the Eastern Algerian basin exhibits a slight symmetrical deepening on both west-east sides of the basin evolving from about 6.1 s TWT to 5.45 s TWT at the central axis of the basin on the R1 anomaly central band (Figure 9). This synthesis of the chrono-lithostratigraphic logs across the EAB shows that the PMU 2 deposited directly on the oceanic crust disappears from the N2 anomaly strip and although it thins by going from R4 to N2 anomalies, evolving from 0.4 s TWT at the basin edges to 0.24 s TWT at the N2 anomaly. This Langhian acoustic unit deposited directly on the oceanic crust from R4 to R3 anomalies is considered as the first acoustic unit overlying the oceanic floor. Similarly, a thinning of the PMU3 thickness is observed along the basin and it evolves from 0.3 s TWT at the basin edges to 0.15 s TWT at the central anomaly (Figure 9). Although from the N2 anomaly, this unit is deposited directly on the oceanic crust as a first Serravalin seismic unit overlying the oceanic floor.

In order to match the magnetic anomalies pattern with the geomagnetic time scale and to test the consistency of our age model (Table 1), we have tried to fit the distribution of identified magnetic anomalies across the strike versus magnetic chron ages as determined in two geomagnetic polarity timescales (Gee and Kent, 2007; Gradstein et al., 2012) assuming a constant spreading rate (Figure 10). These two scales are used to help identify the various age-matching possibilities. Our results show that the uncertainties in the ages (typically of 100 to 200 kyrs, Table 1) are of the same order as the duration of the polarity subchrons (Figure 10), which prevents us from correlating the chrons or sub-chrons exactly with the magnetic anomaly bands. By adding also that the periodicity of magnetic inversions is highly variable during Langhian and Serravalian times and some inversions are so short that they could be missed completely when looking at seafloor anomalies.

However, this result likely means that the assumption of a constant spreading rate is a too strong approximation. For instance, pulses of oceanic spreading after the rifting phase have been identified in the Tyrrhenian back-arc basin, with changes in spreading rates of up to a factor of 3,

resulting from the tearing and fragmentation of the subducting lithosphere, forming slab windows. Such fast changes in spreading rates may well explain why the Langhian-Serravalian polarity chrons cannot be fitted to the spatial distribution of magnetic anomalies in the EAB in absence of data allowing their dating.

Despite the uncertainties inherent to the lack of drilling, our tentative age model built on simple hypotheses on sedimentation and accretion rates supports that the opening of the Eastern Algerian basin (EAB) started during the Middle Miocene for about 2.5 Myr between middle Langhian and middle Serravallian times, i.e. later than assumed in most existing models of opening of the western Mediterranean sea.

5.2 Genetic links between fast block rotation, onset of collision and slab tearing

We have shown that seafloor paleobathymetry (Figure 8 a), pre-Messinian thickness changes (Figure 8 b) and magnetization fabric of the basement (Figure 6) converge to consistently indicate the formation of an ocean seafloor spreading center in the EAB with a rotation pole located near 39°02'N and 05°18'E. The 50-70° clockwise rotation of the GALB (Figure 11b-c) from middle Langhian to middle Serravalian, i.e. in less than 2.5 Myr, recalls similar rotational and migration patterns of back-arc spreading centers within a few million years described in other back-arc settings such as in the North Fiji (Auzende et al., 1988) and Lau basins (Taylor et al., 1996). Their formation is well explained by models of back-arc opening controlled by large transcurrent faults and slab tears (e.g., Fournier et al., 2004; Schellart et al., 2002; Schellart and Moresi, 2013). Such migration is made possible by successive propagation of discrete seafloor spreading centers, producing a magnetization fabric similar to that of mid-oceanic ridges (Taylor et al., 1996), but without ridge segmentation in our case study, possibly due to the reduced size of the EAB oceanic ridge (~220 km long, Figure 6).

In our case study, the hypothesis of slab tearing is strongly supported by the structures of continental margins on both sides of the AB basin. Indeed, recent studies of the westernmost Algerian margin (Badji et al., 2015) and of the central Betics (Mancilla et al., 2013) have shown that the southern and northern margins of the Balearic and Alboran basins are characterized by an abrupt transition between continental and oceanic domains, in agreement with a STEP-fault (Subduction-Transform-Edge-Propagator) origin (Govers and Wortel, 2005). This interpretation is also supported by tomographic studies which depict a northward dipping slab, detached from the continental crust, at depths between 250 and 660 km under the Algerian basin (Fichtner and Villaseñor, 2015).The kinematic evolution proposed agrees with the hypothesis of a decoupling between the Balearic and Sardinian rollback systems along the NBFZ, accommodated by vertical lithosphere tearing forming two slab segments (van Hinsbergen et al., 2014). During this initial stage, the slab sinking has produced asthenospheric rise to the base of the fore-arc, contributing to the collapse of a previous orogen system and explaining the high-temperature Alboran and Kabylides metamorphism and widespread exhumation of subcontinental mantle in latest Oligocene-Early Miocene times (van Hinsbergen et al., 2014, and references therein). Later on, i.e. during middle-late Miocene, the westward propagation of slab tear has enhanced subcontinental-edge delamination and associated sub-lithospheric mantle upwelling explaining the post-collisional magmatism along the Algerian and Alboran margins (Booth-Rea et al., 2007; Chazot et al., 2017; Hidas et al., 2019; Roure et al., 2012 and references therein).

The resulting kinematic model (Figure 11) can be divided in three main stages: (1) the birth of a first basin by crustal stretching accommodating the southern drift of the Kabylian blocks by slab rollback between ~23 and ~15 Ma, (2) the fast opening of a fan-shaped oceanic basin (EAB) between ~15.2 and ~12.7 Ma by an clockwise rotation of the GALB promoted by a first stage of Tethyan westward slab tearing, and (3) an eastward translation and fragmentation of the GALB between ~13 and ~8 Ma promoted by a second stage of Tethyan slab tearing propagating westwards. A striking difference of our kinematic model compared to previous scenarios (Figure 2) is that the seafloor spreading of the EAB post-dates the counterclockwise rotation of Sardinia to the east and the collision of Lesser Kabylia with Africa to the south. Another important change compared to many recent kinematic models (D'Acremont et al., 2020; Do Couto et al., 2016; Romagny et al., 2020) is that the position of the Greater Alboran block (GALB) and the subduction front is located more to the east at 20-16 Ma (Figure 11a-b), as assumed by Mauffret et al. (2004). Whereas, the SE slab rollback exerted a dominant tectonic control between 23 and 16 Ma, while lateral slab tear and westward slab rollback were the driving mechanisms from 16 to 8 Ma.

5.3 Implications for the evolution of back-arc domains influenced by slab tearing

The onset of the EAB opening coincides with the collision of the Kabylian blocks with Africa, but also with the end of transform movements along the NBFZ and CFZ faults and of the opening of the Valencia Trough (Figure 11; (Pellen et al., 2016 and references therein), thus signing a major tectonic and kinematic change in the western Mediterranean at around 16-15 Ma. The diachronicity of opening of the AB and LP basins was not clearly established until now (Figure 2): our study provides strong support for a younger age in the AB and explains why a significantly higher average heat flow is found in this basin compared to the LP one (Poort et al., 2020). While the heat flow is clearly increasing west, the EAB further supports a fast westward drift of the Alboran microplate, and that the WAB is younger than the EAB.

As a whole, our kinematic reconstruction supports a westward displacement of the subduction front of ca. 650 km from ~16 to ~8 Ma (Figure 11b-c-d), corresponding to a lateral finite motion similar to the one hypothesized by (Mauffret et al., 2004). This implies mean slab retreat velocity and full spreading rate of ca. 8 cm/yr, a value comparable to the mean one computed for the Tyrrhenian Sea (Guillaume et al., 2010), and references therein). The relatively fast seafloor spreading rates and short life span determined in this study (Table 1) are in agreement with values found in back-arc settings influenced by additional forces such as slab-pull or anomalous upwelling (Macleod et al., 2017). Indeed, the half-spreading rate of the EAB is estimated to be 3.7 ± 0.5 cm/yr (Table 1), which is typically the rate found in extinct/active microplate or fragmented plate spreading ridges, but appears to be higher than those found in "classical" back-arc basin spreading ridges (Hinschberger et al., 2001; Macleod et al., 2017; Müller et al., 2008). This is also true for sedimentation rates (ca. 0.5 ± 0.1 mm/yr) and ridge relief (ca. 2 km) which appear to be relatively high compared to more linear and larger back-arc basins (Auzende et al., 1988; Hinschberger et al., 2001; Macleod et al., 2017; Taylor et al., 1996). The change from collision of the KB at 19-17 Ma to a perpendicular subduction front later on may have exerted a torque on the upper plate microplate, explaining a rapid vertical axis rotation in the fore-arc and the increase of arc curvature (Figure 11). The EAB opening could have been also enhanced by additional heat sources, such as those arising from toroidal asthenospheric mantle flows in the case of narrow slabs (e.g., (Jolivet et al., 2009; Livermore, 2003; Schellart and Moresi, 2013). In

some way, this geodynamic setting mimics the case of convergent plate margins with a lateral transition from collision to subduction (Wallace et al., 2005).

Another important consequence of our kinematic reconstruction concerns the formation of continental fragments and the role of slab dynamics in their dispersal. Obviously, the tectonic evolution of the AB basin has resulted into the splitting of an initially greater Alboran block into several pieces that were first formed during the southward rollback of the slab (Figure 11a, b) and then reworked and fragmented again during the westward rollback phase (Figure 11c, d). This process is interpreted to be linked with rapid changes of complex subduction dynamics (van den Broek and Gaina, 2020). That is exactly the situation in the present case study at 16-15 Ma, at the moment when the Tethyan slab began to tear by bilateral propagation (Figure 11b-c), thus triggering dispersal of small pieces of continental crust and significant stretching of the GALB by a fast westward rollbak (Figure 11c-d). Even though, The Yusuf-Habibas ridge (YHR) located at the western end of the margin (Figure 11b-c) is formed by a basement block belonging to the Greater Alboran block (Medaouri et al., 2014).

Numerical experiments also suggest that break-up of the upper plate is favored by narrow, inherited weak zones and viscosity contrasts in the crust (van den Broek et al., 2020). Although we lack constraints on the rheology of the GALB, the fact that a narrow slab width promotes a high trench migration rate near lateral slab edges (Schellart et al., 2007) is likely an important reason to explain why the break-up and splitting of the GALB into many small pieces were so efficient. Indeed, narrow slab rollback promotes toroidal mantle flow and high basal shear stresses induced by velocity gradients, resulting in high trench-normal deviatoric tension in the back-arc domain (Mascle and Martin, 1990).

Finally, whether the first basin formed at the rear of the southward rollback stage (i.e., 20-16 Ma, Figure 11b) was continental or oceanic remains unclear (Platt and Vissers, 1989; Do Couto et al., 2016; Platt et al., 2006; Platt and Vissers, 1989; Romagny et al., 2020). This former back-arc domain has been completely reworked later on and may be seen as a continental-type back-arc basin similar to the Aegean extensional domain, characterized by the development of extensional basins (Mascle and Martin, 1990) and by exhumation of metamorphic rocks by detachment faulting, a process controlled at first order by the southward Hellenic trench retreat (Brun and Sokoutis, 2010; Jolivet et al., 2013). The same question is posed regarding the present-day WAB (Figure 11c-d). Although seismic refraction studies indicate an oceanic-type basement (Leprêtre et al., 2013), the contrasting pattern of magnetic anomalies between EAB and WAB basins (Figure 6a) remains to be explained and likely indicates a major change in the way back-arc opening worked after the emplacement of the EAB oceanic basement. The exact nature and mode of formation of the WAB thus need to be accurately investigated to better assess the late stage of opening of the AB basin. More generally, the precise spatial and temporal relationships among the various phases of convergence and extension identified or postulated within the Alboran and Algero-Balearic domains, as well as the amount and timing of slip partitioning onto STEP-faults (e.g., D'Acremont et al., 2020; Jolivet et al., 2021, Platt et al., 2013; Romagny et al., 2020) has not reached a consensus yet. More studies using denser geophysical data and linking land and sea studies are needed to unravel this question.

6 Conclusions

Based on a correlation of deep seismic reflection lines and magnetic anomalies, we show that the opening of the Eastern Algerian basin (EAB) occurred in Langhian-Serravalian times, i.e. after the Corsica-Sardinia block rotation and the collision of the Lesser Kabylia block with Africa, giving rise to a fan-shaped magnetic pattern including 6 magnetic inversions distributed symmetrically from a central negative anomaly. We identify a large paleo-relief covered by pre-Messinian units, featuring an intermediate to fast spreading ridge system emplaced during about 2.45 ± 0.18 Myr, with a half-spreading rate of 3.7 ± 0.5 cm/yr midway from the rotation pole. This fast opening, oblique or orthogonal to the Africa-Eurasia plate convergence, is assumed to be primarily driven by a westward Tethyan slab rollback and tearing. Accordingly, we reassess the kinematic models of the Algero-Balearic basin proposed until now into three main stages: (1) the birth of a first basin by crustal stretching accommodating the southern drift of the Kabylian blocks by a southward Tethyan slab rollback between ~23 and ~15 Ma, (2) the fast opening of a fan-shaped oceanic basin (EAB) between 15.2 and 12.7 Ma by a clockwise rotation of the GALB (Greater Alboran block) promoted by a first stage of westward slab tearing, and (3) a translation and fragmentation of the GALB between ~13 and 8 Ma promoted by a second stage of westward Tethyan slab tearing. This process of slab segmentation and separation, as proposed in recent geodynamic models of the western Mediterranean Sea (van Hinsbergen et al., 2014, 2020), offers the most likely mechanism to explain the two last stages of opening of the Algero-Balearic domain. The EAB case study illustrates how collision-induced rotations following slab rollback and associated increase of arc curvature may lead to complex back-arc rifting systems with highly variable geometry and strain rates and may foster fore-arc fragmentation in a short geological time scale (Guillaume et al., 2010; Wallace et al., 2005; van den Broeke and Gaina, 2020; van Hinsbergen et al., 2020).

Acknowledgments and data availability statement

The authors wish to gratefully thank Angelo Camerlenghi, Anna del Ben, Edy Forlin, Johanna Lofi and Fadel Raad for providing access to various seismic profiles and valuable feedback and comments that contributed to improve this work. Seismic interpretation and isopach mapping was facilitated by IHS Markit's Kingdom Suite and Schlumberger's Petrel softwares respectively, provided on an academic license. We also acknowledge the support of ISblue project-Interdisciplinary graduate school for the blue planet (ANR-17-EURE-0015)- co-funded by a grant from the French government under the program "Investissements d'Avenir".

Data for this research are not publicly available to respect terms of use for data obtained in agreement with Sonatrach. Various Datasets for this research are included in this paper (and its supplementary information files): [Arab, M., Rabineau, M., Déverchère, J., Bracene, R., Belhai, D., Roure, F., et al. (2016). Tectonostratigraphic evolution of the eastern Algerian margin and basin from seismic data and onshore-offshore correlation. Marine and Petroleum Geology, 77, 1355–1375. https://doi.org/10.1016/j.marpetgeo.2016.08.021; Bouyahiaoui, B., Sage, F., Abtout, A., Klingelhoefer, F., Yelles-Chaouche, K., Schnurle, P., et al. (2015). Crustal structure of the eastern Algerian continental margin and adjacent deep basin: implications for late Cenozoic geodynamic evolution of the western Mediterranean. Geophysical Journal International, 201(3), 1912–1938. https://doi.org/10.1093/gji/ggv102; Mihoubi, A., Schnürle, P., Benaissa, Z., Badsi, M., Bracene, R., Djelit, H., et al. (2014). Seismic imaging of the eastern Algerian margin off Jijel: integrating wide-angle seismic modelling and multichannel seismic pre-stack depth migration.

Geophysical Journal International, 198(3), 1486–1503. https://doi.org/10.1093/gji/ggu179; Graindorge, D., Sage, F., & Klingelhoefer, F. (2009). SPIRAL cruise, L'Atalante R/V. https://doi.org/10.17600/9010050].

Datasets for this research are described in this paper: [Cope, M. J. (2003). Algerian licensing round may offer opportunity for exploration plays in deep offshore frontier. First Break, 21(7). https://doi.org/0.3997/1365-2397.21.7.25550; Finetti, I., & Morelli, C. (1972). Wide scale digital seismic exploration of the Mediterranean sea. Wide Scale Digital Seismic Exploration of the Mediterranean Sea; Graindorge, D., Sage, F., & Klingelhoefer, F. (2009). SPIRAL cruise, L'Atalante R/V. https://doi.org/10.17600/9010050; Mauffret, Alain. (2007). The Northwestern (Maghreb) boundary of the Nubia (Africa) Plate. Tectonophysics, 429(1), 21–44. https://doi.org/10.1016/j.tecto.2006.09.007].

Figure Captions

Figure 1. Structural map of the Western Mediterranean region displaying the main offshore basins (Algerian basin, Alboran Sea, Liguro-Provençal Basin, Tyrrhenian Sea and Valencia Trough), Cenozoic structures and distribution of the AlKaPeCa domain on land, modified after (Arab et al., 2016b; Leprêtre et al., 2018; Pellen et al., 2016). Digital topography is based on the GEBCO 20 (IOC-IHO) online database combined with the bathymetry from GeoMapApp (www.geomapapp.org; (Ryan et al., 2009) for the offshore region. Abbreviations: LK & GK = Lesser & Greater Kabylia, respectively; CAL= Calabria; Pe = Peloritan; NBFZ = North Balearic Fracture Zone; CFZ = Central Fracture Zone; EBE = Emile Baudot Escarpment, ME= Mazaron Escarpment; JF = Jebha Fault; NF = Nekor Fault; YR= Yusuf Ridge; YE= Yusuf Escarpment.

Figure 2. Simplified sketches of the main conflicting kinematic models featuring the assumed mode and timing of opening of the Algerian basin within the Western Mediterranean Sea. Redrawn from (a) (Schettino and Turco, 2006), (b) (Martin, 2006), (c) (Mauffret et al., 2004) and (d) Cohen (1980), later re-used by Driussi et al. (2015). Time spans considered are shown in the upper left side of each scenario. Note that except Model c, all models are predicting an opening of the East Algerian basin (EAB) before 15 Ma, i.e. roughly synchronously to the opening of the Liguro-Provençal basin and to the drift of the Corsica-Sardinia block. See text for details.

Figure 3. Litho-stratigraphic correlation of the Oligo-Miocene series that crops out onshore and extrapolation to the offshore domain for identifying the pre-Messinian units, modified from Arab et al. (2016b). The litho-stratigraphic section of Sidi Ali Ben Toumi (Soummam basin) and Collo and the related Miocene ages are from (Carbonnel and Courme-Rault, 1997). The attributed stratigraphic limits onshore are documented from (Bouillin, 1986), (Courme-Rault, 1985) and (Carbonnel and Courme-Rault, 1997). The Serravallian of Soummam basin is described at Sidi Aich (Bejaia) while the Tortonian is described at Oued Ghir by (Courme-Rault, 1985). 7a: Serravallian of Sidi Aich area, 7b: Tortonian of Oued Ghir area.

Figure 4. (a) Morphological map of northern Algeria and the Algerian basin with geological units onshore and positions of seismic lines offshore. The geological map represents the main units of the Maghrebides and Tell-Atlas belts after Leprêtre et al. (2018). Stars are Ocean Drilling Program (976, 977, 978, 974 and 974) and commercial drilling sites. CB= Cape Bougaroun; CDF= Cap de Fer; CEO= Cape El-Ouana. (b) Location map of the eastern Algerian margin and basin displaying the seismic lines used in this work. "L": acquired by Western Geco (2000-2002; Cope, 2003);

"SPI": acquired during the SPIRAL Project (Graindorge et al., 2009), including five wide-angle seismic profiles with positions of OBS; "ALE" (Total) and "MS" (MCS profiles acquired by OGS (1972 - 1979 R/V Marsili), (Finetti and Morelli, 1972) (see Data Repository for more details).

Figure 5. Representative multichannel seismic section (off Bejaia, see location on Figure 4) displaying the seismostratigraphic framework of the EAB (see location on Figure 4), with main seismic units and major reflectors, and correlation with mean interval velocities (modified from Arab et al. (2016a, 2016b)), and (Leroux et al., 2019). Assumed ages, litho-stratigraphic correlations and Transgressive-Regressive (T-R) sequences of the Miocene series are extrapolated from onland observations to the offshore domain after Arab et al. (2016a,b).

Figure 6. (a) Structural scheme of the magnetic substratum of the Algerian basin. Offshore, the background represents the reduced-to-the-pole (RTP) magnetic anomalies with the interpretation of the main fault systems (modified after Medaouri et al. (2014) and our interpretation of magnetic stripes in the eastern Algerian basin (EAB); (b) Zoom on the EAB displaying regularly spaced N-S to NW–SE magnetic anomalies interpreted as black and white stripes representing periods of normal and reverse magnetic polarity, respectively. R, N= Normal and Reverse magnetic polarities; W for West, E for East; OT= Oceanic Transform Fault; SC= Seafloor Spreading center; STEP = Subduction-Transform-Edge-Propagator; CF and CP= Cap de Fer and Cape Bougaroun; Red star is the approximate position of the rotation pole; Grey dotted line represents the midway path from the rotation pole; Transitional domain of Sardinia from Afilhado et al. (2015).

Figure 7. Crossing seismic sections between seismic lines of different quality (a,b,c,d,e) and one seismic section (f) highlighting the evolution of pre-Messinian units overlying the oceanic crust and their thickness above the fan-shaped magnetization zone of the EAB. Black dots are internal reflectors within the basement. Location of the seismic lines is shown on the inset map.

Figure 8. Seismic-based time-structure maps of (a) Horizon B (top basement) and (b) Horizon R5 - Horizon B (thickness of pre-salt sequence) in the East Algerian basin (EAB) The dotted grey lines locates the transition between continental, transitional and oceanic domains (Aïdi et al., 2018; Bouyahiaoui et al., 2015; Mihoubi et al., 2014). The north-verging ramps displaying the Quaternary inversion of the margin and the normal faults are taken from Arab et al. (2016b), while the basement grids off Sardinia and the Balearic Islands are taken from Driussi et al. (2015) and Leroux et al. (2019). The semi-transparent black lines delimits the R/N magnetic stripes. R, N = Normal and Reverse magnetic polarities; W for West, E for East.

Figure 9. Synthesis of chrono-lithostratigraphic logs across the EAB. Depths are in seconds two-way travel time (s twt) below sea-level. The mean thickness of each unit is obtained at the crossing points of the seismic sections in the deep offshore (Letters A-G and A'-F', inset). N, R = Normal and Reverse polarities, respectively; W for West, E for East. Dashed black line locates the transition between continental and oceanic domains (after (Bouyahiaoui et al., 2015; Mihoubi et al., 2014). Bold gray lines represent the main profiles sections used. R1 is assumed to represent the central, youngest magnetic anomaly according to the magnetic pattern of the EAB, whereas R4W and R4E are assumed to be the oldest ones where the first oceanic crust emplaced (Figure 6). East of R1, the low quality of seismic data prevents us from separating pre-Messinian units above the basement, except at F' (Anomaly N1e).

Figure 10. Sketch showing the correlation between the predicted ages (top) calculated from the hypothesis discussed in Table 1 (bottom) and the chrons (down) taken from the Geomagnetic Polarity Timescales from (Gee and Kent, 2007) and Gradstein et al. (2012) and the first deposits overlying the oceanic crust (PMU2 or PMU3) assuming a constant spreading rate during Langhian-Serravalian times. Red hatched rectangles represent the ages uncertainties (see Table 1 for details). The prefix 'C' corresponds to chron sub-divided into two intervals of predominantly normal 'n' and reverse 'r' polarity. The shorter polarity chrons are referred to as subchrons which are identified by appending, from the youngest to the oldest ones, '.1', '.2' to the polarity chron name, and by adding 'n' or 'r' for normal or reverse polarity respectively.

Figure 11. Kinematic reconstruction of the Algero-Balearic domain with the main paleogeographic features of the Mediterranean sea between 20 and 8 Ma. Modified after Mauffret et al. (2004), Medaouri et al. (2014), van Hinsbergen et al. (2014, 2020); d'Acremont et al. (2020). Shape, size and distribution of abandoned continental fragments of the GALB (Great Alboran Block) are poorly constrained and must therefore be considered as hypothetical.

(a) ~20 Ma: the southward Tethyan rollback is ending, collision of Kaylian blocks with Africa is beginning, in a way similar to the present-day situation of Crete relative to Africa, and the back-arc basin is submitted to radial extension, in a way similar to the present-day Aegean Sea.

(b) ~16 Ma: the Corsica-Sardinia block has reached its present-day position, the LP oceanic basin is formed, the collision of Kaylian blocks with Africa is ending, the GALB is highly stretched in the N-S dominant strike, possibly leading to a highly thinned continental crust or exhumed mantle in the forearc; the Tethyan slab tearing has started, thus triggering the birth of a first accretionary system along the North Balearic Fracture zone (NBFZ) and the emplacement of post-collisional magmatism and mantle delamination in the Lesser Kabylia margin.

(c) ~12 Ma : the EAB is formed by progressive westward migration of the seafloor spreading axis and a change of strike from NW to NNW; the GALB is stretched in the W-E direction and is guided by the STEP faults north (EBE) and south (Al).

(d) ~8 Ma: the slab tearing has propagated westward, thus promoting the westward rollback and transfer of the GALB by STEP-faults along the Betic and Algerian margins (Btc and RT respectively) and the formation of the narrowest part of the Algero-Balearic oceanic back-arc basin (WAB).

Abbreviations: Af - Eu Conv= Africa-Eurasia convergence; Alp= Alpujarride units; Cal= Calabria terranes; Cal & Bal-SZ= Calabrian & Balearic subduction zones; CFZ= Central Fracture Zone; NBFZ= North Balearic Fracture Zone; DoC= Dorsale Calcaire; EAB= Eastern Algerian Basin; EBE: Emile Baudot Escarpment; GALB= Greater Alboran Block; Gho= Ghomaride units; GoV= Gulf of Valencia; HH= Hannibal High; LK & GK= Lesser & Greater Kabylia; LPB= Liguro-Provençal Basin; Mal = Malaguide units; NeF= Nevado - Filabride unit; Pe= Peloritani terranes; RoP= Ronda Peridotite; Seb= Sebtides (including Beni Boussera peridotite); SMB = South Menorca Block. STEP Fault= Subduction-Transform-Edge-Propagator, also called tear fault (Al: Algerian; TA: Tunisan; RT: Rif-Tell; Btc: Betic); WAB= Western Algerian Basin; AlB= Alboran Block.

References

Abbassene, F., Chazot, G., Bellon, H., Bruguier, O., Ouabadi, A., Maury, R. C., et al. (2016). A 17Ma onset for the post-collisional K-rich calc-alkaline magmatism in the Maghrebides: Evidence from Bougaroun (northeastern Algeria) and geodynamic implications. Tectonophysics, 674, 114–134. https://doi.org/10.1016/j.tecto.2016.02.013

Afilhado, A., Moulin, M., Aslanian, D., Schnürle, P., Klingelhoefer, F., Nouzé, H., et al. (2015). Deep crustal structure across a young passive margin from wide-angle and reflection seismic data (The SARDINIA Experiment) – II. Sardinia's margin. Bulletin de La Société Géologique de France, 186(4–5), 331–351 https://doi.org/10.2113/gssgfbull.186.4-5.331

Aïdi, C., Beslier, M.-O., Yelles-Chaouche, A. K., Klingelhoefer, F., Bracene, R., Galve, A., et al. (2018). Deep structure of the continental margin and basin off Greater Kabylia, Algeria – New insights from wide-angle seismic data modeling and multichannel seismic interpretation. Tectonophysics, 728–729, 1–22. https://doi.org/10.1016/j.tecto.2018.01.007

Aïte, M. O., & Gélard, J. P. (1997). Post-collisional palaeostresses in the central Maghrebides (Great Kabylia, Algeria). Bull. Soc. Géol. Fr., pp. 423–436.

Alvarez, W., Cocozza, T., & Wezel, F. C. (1974). Fragmentation of the Alpine orogenic belt by microplate dispersal. Nature, 248(5446), 309–314. https://doi.org/10.1038/248309a0

Andrieux, J., Fontbote, J.-M., & Mattauer, M. (1971). Sur un modele explicatif de l'arc de Gibraltar. Earth and Planetary Science Letters, 12(2), 191–198. https://doi.org/10.1016/0012-821X(71)90077-X

Arab, M., Belhai, D., Granjeon, D., Roure, F., Arbeaumont, A., Rabineau, M., et al. (2016). Coupling stratigraphic and petroleum system modeling tools in complex tectonic domains: case study in the North Algerian Offshore. Arabian Journal of Geosciences, 9(4), 289. https://doi.org/10.1007/s12517-015-2296-3

Arab, M., Rabineau, M., Déverchère, J., Bracene, R., Belhai, D., Roure, F., et al. (2016). Tectonostratigraphic evolution of the eastern Algerian margin and basin from seismic data and onshore-offshore correlation. Marine and Petroleum Geology, 77, 1355–1375. https://doi.org/10.1016/j.marpetgeo.2016.08.021

Auzende, J.-M., Bonnin, J., & Olivet, J.-L. (1973). The origin of the western Mediterranean basin. Geological Society of London, 129, 607–620.

Auzende, J.-M., Lafoy, Y., & Marsset, B. (1988). Recent geodynamic evolution of the north Fiji basin (southwest Pacific). Geology, 16(10), 925–929. https://doi.org/10.1130/0091-7613(1988)016<0925:RGEOTN>2.3.CO;2

Ayala, C., Bohoyo, F., Maestro, A., Reguera, M. I., Torne, M., Rubio, F., et al. (2016). Updated Bouguer anomalies of the Iberian Peninsula: a new perspective to interpret the regional geology. Journal of Maps, 12(5), 1089–1092. https://doi.org/10.1080/17445647.2015.1126538

Badji, R., Charvis, P., Bracene, R., Galve, A., Badsi, M., Ribodetti, A., et al. (2015). Geophysical evidence for a transform margin offshore Western Algeria: a witness of a subduction-

transform edge propagator? Geophysical Journal International, 200(2), 1029–1045. https://doi.org/10.1093/gji/ggu454

Bayer, R., Le Mouel, J. L., & Le Pichon, X. (1973). Magnetic anomaly pattern in the western mediterranean. Earth and Planetary Science Letters, 19(2), 168–176. https://doi.org/10.1016/0012-821X(73)90111-8

Biju-Duval, B., Dercourt, V., & Le Pichon, X. (1977). From the Tethys ocean to the Mediterranean sea: a plate tectonic model of the evolution of the western Alpine system. In: The Structural History of the Mediterranean Basin, pp. 143–164.

Boccaletti, M., & Guazzone, G. (1974). Remnant arcs and marginal basins in the Cainozoic development of the Mediterranean. Nature, 252(5478), 18–21. https://doi.org/10.1038/252018a0

Booth-Rea, G., Ranero, C. R., Martínez-Martínez, J. M., & Grevemeyer, I. (2007). Crustal types and Tertiary tectonic evolution of the Alborán sea, western Mediterranean. Geochemistry, Geophysics, Geosystems, 8(10). https://doi.org/10.1029/2007GC001639

Bouillin, J. P. (1986). Le bassin maghrebin; une ancienne limite entre l'Europe et l'Afrique a l'ouest des Alpes. Bulletin de La Société Géologique de France, II(4), 547–558. https://doi.org/10.2113/gssgfbull.II.4.547

Bouillin, J.-P., & Raoult, J.-F. (1971). Presence sur le socle kabyle du Constantinois d'un olistostrome lie au charriage des flyschs; le Numidien peut-il etre un neo-autochtone? Bulletin de La Société Géologique de France, S7-XIII(3–4), 338–362. https://doi.org/10.2113/gssgfbull.S7-XIII.3-4.338

Bouillin, J.-P. & Université Pierre et Marie Curie (Paris / 1971-2017). (1977). Géologie alpine de la petite Kabylie dans les régions de Collo et d'El Milia (Algérie) (Doctoral dissertation). Université Pierre et Marie Curie, France.

Bouyahiaoui, B., Sage, F., Abtout, A., Klingelhoefer, F., Yelles-Chaouche, K., Schnurle, P., et al. (2015). Crustal structure of the eastern Algerian continental margin and adjacent deep basin: implications for late Cenozoic geodynamic evolution of the western Mediterranean. Geophysical Journal International, 201(3), 1912–1938. https://doi.org/10.1093/gji/ggv102

van den Broek, J. M., & Gaina, C. (2020). Microcontinents and Continental Fragments Associated With Subduction Systems. Tectonics, 39(8), e2020TC006063. https://doi.org/10.1029/2020TC006063

van den Broek, J. M., Magni, V., Gaina, C., & Buiter, S. J. H. (2020). The Formation of Continental Fragments in Subduction Settings: The Importance of Structural Inheritance and Subduction System Dynamics. Journal of Geophysical Research: Solid Earth, 125(1), e2019JB018370. https://doi.org/10.1029/2019JB018370

Brun, J.-P., & Sokoutis, D. (2010). 45 m.y. of Aegean crust and mantle flow driven by trench retreat. Geology, 38(9), 815–818. https://doi.org/10.1130/G30950.1

Camerlenghi, A., Accettella, D., Costa, S., Lastras, G., Acosta, J., Canals, M., & Wardell, N. (2008). Morphogenesis of the SW Balearic continental slope and adjacent abyssal plain, Western Mediterranean Sea. International Journal of Earth Sciences, 98(4), 735. https://doi.org/10.1007/s00531-008-0354-8

Carbonnel, G., & Courme-Rault, M.-D. (1997). Ostracodes miocènes d'Algérie (systématique, biostratigraphie, distribution palinspatique). Publications du musée des Confluences, 1(1). Retrieved from https://www.persee.fr/doc/mhnly_1285-882x_1997_mon_1_1

Carey, S. W. (1955). The orocline concept in geotectonics- Part I. Papers and Proceedings of the Royal Society of Tasmania, 89, 255–288.

Carminati, E, Wortel, M. J. R., Spakman, W., & Sabadini, R. (1998a). The role of slab detachment processes in the opening of the western–central Mediterranean basins: some geological and geophysical evidence. Earth and Planetary Science Letters, 160(3), 651–665. https://doi.org/10.1016/S0012-821X(98)00118-6

Carminati, E, Wortel, M. J. R., Meijer, P. T., & Sabadini, R. (1998b). The two-stage opening of the western–central Mediterranean basins: a forward modeling test to a new evolutionary model. Earth and Planetary Science Letters, 160(3), 667–679. https://doi.org/10.1016/S0012-821X(98)00119-8

Carminati, Eugenio, Lustrino, M., & Doglioni, C. (2012). Geodynamic evolution of the central and western Mediterranean: Tectonics vs. igneous petrology constraints. Tectonophysics, 579, 173–192. https://doi.org/10.1016/j.tecto.2012.01.026

Chazot, G., Abbassene, F., Maury, R. c., Déverchère, J., Bellon, H., Ouabadi, A., & BOSCH, D. (2017). An overview on the origin of post-collisional Miocene magmatism in the Kabylies (northern Algeria): Evidence for crustal stacking, delamination and slab detachment. Journal of African Earth Sciences, 125, 27–41. https://doi.org/10.1016/j.jafrearsci.2016.10.005

Chertova, M. V., Spakman, W., Geenen, T., Berg, A. P. van den, & Hinsbergen, D. J. J. van. (2014). Underpinning tectonic reconstructions of the western Mediterranean region with dynamic slab evolution from 3-D numerical modeling. Journal of Geophysical Research: Solid Earth, 119(7), 5876–5902. https://doi.org/10.1002/2014JB011150

Cohen, C. R. (1980). Plate tectonic model for the oligo-miocene evolution of the western Mediterranean. Tectonophysics, 68(3–4), 283–311. https://doi.org/10.1016/0040-1951(80)90180-8

Cohen, K. M., Finney, S. C., Gibbard, P. L., & Fan, J.-X. (2013). The ICS International Chronostratigraphic Chart. Episodes, 36(3), 199–204. https://doi.org/10.18814/epiiugs/2013/v36i3/002

Cope, M. J. (2003). Algerian licensing round may offer opportunity for exploration plays in deep offshore frontier. First Break, 21(7). https://doi.org/0.3997/1365-2397.21.7.25550

Courme-Rault, M.-D. (1985). Stratigraphie du miocène et chronologie comparée des déformations suivant deux transversales des atlasides orientales (Algérie, Sicile): Texte imprimé (Doctoral dissertation). Université d'Orléans, France.

D'Acremont, E., Lafosse, M., Rabaute, A., Teurquety, G., Do Couto, D., Ercilla, G., et al. (2020). Polyphase Tectonic Evolution of Fore-Arc Basin Related to STEP Fault as Revealed by Seismic Reflection Data From the Alboran Sea (W-Mediterranean). Tectonics, 39(3). https://doi.org/10.1029/2019TC005885

Dal Cin, M., Ben, A., Mocnik, A., Accaino, F., Geletti, R., Wardell, N., et al. (2016). Seismic imaging of Late Miocene (Messinian) evaporites from Western Mediterranean back-arc basins. Petroleum Geoscience, 22, petgeo2015-096. https://doi.org/10.1144/petgeo2015-096

Déverchère, J., Medaouri, M., Beslier, M.-O., Arab, M., Graindorge, D., Bracene, R., et al. (15-16 March). How does tectonic inversion initiate? Insights from the Algerian margin case study. Presented at the AAPG GTW "Alpine folded belts and extensional basins: Exploring in the Mediterranean," Granada, Spain, 5-16 March.

Dewey, J. F., Helman, M. L., Knott, S. D., Turco, E., & Hutton, D. H. W. (1989). Kinematics of the western Mediterranean. Geological Society, London, Special Publications, 45(1), 265–283. https://doi.org/10.1144/GSL.SP.1989.045.01.15

Dewey, John F., Pitman, W. C., Ryan, W. B. F., & Bonnin, J. (1973). Plate Tectonics and the Evolution of the Alpine System. GSA Bulletin, 84(10), 3137–3180. https://doi.org/10.1130/0016-7606(1973)84<3137:PTATEO>2.0.CO;2

Dix, C. H. (1955). Seismic velocities from surface measurements. GEOPHYSICS, 20(1), 68–86. https://doi.org/10.1190/1.1438126

Do Couto, D., Gorini, C., Jolivet, L., Lebret, N., Augier, R., Gumiaux, C., et al. (2016). Tectonic and stratigraphic evolution of the Western Alboran Sea Basin in the last 25Myrs. Tectonophysics, C(677–678), 280–311. https://doi.org/10.1016/j.tecto.2016.03.020

Driussi, O., Briais, A., & Maillard, A. (2015). Evidence for transform motion along the South Balearic margin and implications for the kinematics of opening of the Algerian basin. Bulletin de La Société Géologique de France, 186(4–5), 353–370. https://doi.org/10.2113/gssgfbull.186.4-5.353

Durand Delga, M. (1980). La Méditerranée occidentale, étapes de sa genèse et problèmes structuraux liés à celle-ci. Mém. Soc. Géol. France, 10, 203–224.

Faccenna, C., Piromallo, C., Crespo-Blanc, A., Jolivet, L., & Rossetti, F. (2004). Lateral slab deformation and the origin of the western Mediterranean arcs. Tectonics, 23(1). https://doi.org/10.1029/2002TC001488

Fichtner, A., & Villaseñor, A. (2015). Crust and upper mantle of the western Mediterranean – Constraints from full-waveform inversion. Earth and Planetary Science Letters, 428, 52–62. https://doi.org/10.1016/j.epsl.2015.07.038

Finetti, I., & Morelli, C. (1972). Wide scale digital seismic exploration of the Mediterranean sea. Wide Scale Digital Seismic Exploration of the Mediterranean Sea.

Fournier, M., Jolivet, L., Davy, P., & Thomas, J.-C. (2004). Back arc extension and collision : an experimental approach of the tectonics of Asia. Geophysical Journal International, 157, 871–889. https://doi.org/10.1111/j.1365-246X.2004.02223.x

Frizon de lamotte, D., Bezar, B. S., Bracène, R., & Mercier, E. (2000). The two main steps of the Atlas building and geodynamics of the western Mediterranean. Tectonics, 19(4), 740–761. https://doi.org/10.1029/2000TC900003

Frizon de Lamotte, D., Crespo-Blanc, A., Saint-Bézar, B., Comas, M., Fernandez, M., Zeyen, H., et al. (2004). TRASNSMED-transect I [Betics, Alboran Sea, Rif, Moroccan Meseta, High

Atlas, Jbel Saghro, Tindouf basin]. Cavazza W., Roure F., Spakman W., Stampfli GM & Ziegler PA (Éds.)–The TRANSMED Atlas-the Mediterranean Region from Crust to Mantle.

De Lamotte, F. de, Bezar, B. S., Bracène, R., & Mercier, E. (2000). The two main steps of the Atlas building and geodynamics of the western Mediterranean. Tectonics, 19(4), 740–761. https://doi.org/10.1029/2000TC900003

Galdeano, A., & Rossignol, J.-C. (1977). Assemblage a altitude constante des cartes d'anomalies magnetiques couvrant l'ensemble du bassin occidental de la Mediterranee. Bulletin de La Société Géologique de France, S7-XIX(3), 461–468. https://doi.org/10.2113/gssgfbull.S7-XIX.3.461

Gattacceca, J., Deino, A., Rizzo, R., Jones, D. S., Henry, B., Beaudoin, B., & Vadeboin, F. (2007). Miocene rotation of Sardinia: new paleomagnetic and geochronological constraints and geodynamic implications. Earth and Planetary Science Letters, 258, 359–377. https://doi.org/10.1016/j.epsl.2007.02.003

Gee, J. S., & Kent, D. V. (2007). 5.12 - Source of Oceanic Magnetic Anomalies and the Geomagnetic Polarity Timescale. In G. Schubert (Ed.), Treatise on Geophysics (pp. 455–507). Amsterdam: Elsevier. https://doi.org/10.1016/B978-044452748-6.00097-3

Gelabert, B., Sàbat, F., & Rodríguez-Perea, A. (2002). A new proposal for the late Cenozoic geodynamic evolution of the western Mediterranean. Terra Nova, 14(2), 93–100. https://doi.org/10.1046/j.1365-3121.2002.00392.x

Gómez de la Peña, L., Ranero, C. R., & Gràcia, E. (2018). The Crustal Domains of the Alboran Basin (Western Mediterranean). Tectonics, 37(10), 3352–3377. https://doi.org/10.1029/2017TC004946

Govers, R., & Wortel, M. J. R. (2005). Lithosphere tearing at STEP faults: response to edges of subduction zones. Earth and Planetary Science Letters, 236(1), 505–523. https://doi.org/10.1016/j.epsl.2005.03.022

Gradstein, F. M., Ogg, J. G., Schmitz, M. D., & Ogg, G. M. (2012). The Geologic Time Scale 2012. Elsevier.

Graindorge, D., Sage, F., & Klingelhoefer, F. (2009). SPIRAL cruise,L'Atalante R/V. https://doi.org/10.17600/9010050

Granado, P., Urgeles, R., Sàbat, F., Albert-Villanueva, E., Roca, E., Muñoz, J. A., et al. (2016). Geodynamical framework and hydrocarbon plays of a salt giant: the NW Mediterranean Basin. Petroleum Geoscience, 22(4), 309–321. https://doi.org/10.1144/petgeo2015-084

Gueguen, E., Doglioni, C., & Fernandez, M. (1998). On the post-25 Ma geodynamic evolution of the western Mediterranean. Tectonophysics, 298(1), 259–269. https://doi.org/10.1016/S0040-1951(98)00189-9

Guillaume, B., Funiciello, F., Faccenna, C., Martinod, J., & Olivetti, V. (2010). Spreading pulses of the Tyrrhenian Sea during the narrowing of the Calabrian slab. Geology, 38(9), 819–822. https://doi.org/10.1130/G31038.1

Haq, B. U., & Schutter, S. R. (2008). A Chronology of Paleozoic Sea-Level Changes. Science, 322(5898), 64–68. https://doi.org/10.1126/science.1161648

Hidas, K., Garrido, C. J., Booth-Rea, G., Marchesi, C., Bodinier, J.-L., Dautria, J.-M., et al. (2019). Lithosphere tearing along STEP faults and synkinematic formation of lherzolite and wehrlite in the shallow subcontinental mantle. Solid Earth, 10(4), 1099–1121. https://doi.org/10.5194/se-10-1099-2019

Hinsbergen, D. J. J. van, Vissers, R. L. M., & Spakman, W. (2014). Origin and consequences of western Mediterranean subduction, rollback, and slab segmentation. Tectonics, 33(4), 393–419. https://doi.org/10.1002/2013TC003349

van Hinsbergen, D. J. J., Vissers, R. L. M., & Spakman, W. (2014). Origin and consequences of western Mediterranean subduction, rollback, and slab segmentation. Tectonics, 33(4), 393–419. https://doi.org/10.1002/2013TC003349

van Hinsbergen, D. J. J., Torsvik, T. H., Schmid, S. M., Maţenco, L. C., Maffione, M., Vissers, R. L. M., et al. (2020). Orogenic architecture of the Mediterranean region and kinematic reconstruction of its tectonic evolution since the Triassic. Gondwana Research, 81, 79–229. https://doi.org/10.1016/j.gr.2019.07.009

Hsu, K., Montadert, L., & et al. (1978). Initial Reports of the Deep Sea Drilling Project, 42 Pt. 1 (Vol. 42 Pt. 1). U.S. Government Printing Office. https://doi.org/10.2973/dsdp.proc.42-1.1978

Jackson, M. P. A., & Hudec, M. R. (Eds.). (2017). Seismic Interpretation of Salt Structures. In Salt Tectonics: Principles and Practice (pp. 364–398). Cambridge: Cambridge University Press. https://doi.org/10.1017/9781139003988.018

Jolivet, L., & Faccenna, C. (2000). Mediterranean extension and the Africa-Eurasia collision. Tectonics, 19(6), 1095–1106. https://doi.org/10.1029/2000TC900018

Jolivet, L., Faccenna, C., & Piromallo, C. (2009). From mantle to crust: Stretching the Mediterranean. Earth and Planetary Science Letters, 285(1), 198–209. https://doi.org/10.1016/j.epsl.2009.06.017

Jolivet, L., Faccenna, C., Huet, B., Labrousse, L., Le Pourhiet, L., Lacombe, O., et al. (2013). Aegean tectonics: Strain localisation, slab tearing and trench retreat. Tectonophysics, 597–598, 1–33. https://doi.org/10.1016/j.tecto.2012.06.011

Jolivet, L., Menant, A., Roche, V., Le Pourhiet, L., Maillard, A., Augier, R., et al. (2021). Transfer zones in Mediterranean back-arc regions and tear faults. Bulletin de La Société Géologique de France, 192(11). https://doi.org/10.1051/bsgf/2021006

Leprêtre, A., Klingelhoefer, F., Graindorge, D., Schnurle, P., Beslier, M. O., Yelles, K., et al. (2013). Multiphased tectonic evolution of the Central Algerian margin from combined wide-angle and reflection seismic data off Tipaza, Algeria. Journal of Geophysical Research: Solid Earth, 118(8), 3899–3916. https://doi.org/10.1002/jgrb.50318

Leprêtre, R., Lamotte, D. F. de, Combier, V., Gimeno-Vives, O., Mohn, G., & Eschard, R. (2018). The Tell-Rif orogenic system (Morocco, Algeria, Tunisia) and the structural heritage of the southern Tethys margin. BSGF - Earth Sciences Bulletin, 189(2), 10. https://doi.org/10.1051/bsgf/2018009

Leroux, E. (2012). Quantification des flux sédimentaires et de la subsidence du bassin Provençal (Doctoral dissertation). Université Européenne de Bretagne, Brest, France. Retrieved from https://archimer.ifremer.fr/doc/00108/21967/

Leroux, E., Daniel, A., Marina, R., Christian, G., Jean-Loup, R., Jeffrey, P., et al. (2019). ATLAS of the stratigraphic markers in the Western Mediterranean with focus on the Messinian, Pliocene and Pleistocene of the Gulf of Lion. FR: CCGM-CGMW. Retrieved from https://doi.org/10.14682/2019GULFLIONATL

Livermore, R. (2003). Back-arc spreading and mantle flow in the East Scotia Sea. In R. D. Larter & P. T. Leat (Eds.), Intra-oceanic subduction systems: tectonic and magmatic processes (pp. 315–331). London: Geological Society of London. Retrieved from http://nora.nerc.ac.uk/id/eprint/16878/

Lofi, J., Déverchère, J., Gaullier, V., Herve, G., Gorini, C., Guennoc, P., et al. (2011). Seismic Atlas of the Messinian Salinity Crisis markers in the Mediterranean and Black Seas. Mém. Soc. Géol. Fr., n.s. (Vol. 179).

Lonergan, L., & White, N. (1997). Origin of the Betic-Rif mountain belt. Tectonics, 16(3), 504–522. https://doi.org/10.1029/96TC03937

Macleod, S., Williams, S., Matthews, K., Müller, D., & Qin, X. (2017). A global review and digital database of large-scale extinct spreading centers. Geosphere, 13, GES01379.1. https://doi.org/10.1130/GES01379.1

Maillard, A., Mauffret, A., Watts, A. B., Torné, M., Pascal, G., Buhl, P., & Pinet, B. (1992). Tertiary sedimentary history and structure of the Valencia trough (western Mediterranean). Tectonophysics, 203(1), 57–75. https://doi.org/10.1016/0040-1951(92)90215-R

Maillard, Agnès, Jolivet, L., Lofi, J., Thinon, I., Couëffé, R., Canva, A., & Dofal, A. (2020). Transfer zones and associated volcanic province in the eastern Valencia Basin: Evidence for a hot rifted margin? Marine and Petroleum Geology, 119, 104419. https://doi.org/10.1016/j.marpetgeo.2020.104419

Malinverno, A., & Ryan, W. B. F. (1986). Extension in the Tyrrhenian Sea and shortening in the Apennines as result of arc migration driven by sinking of the lithosphere. Tectonics, 5(2), 227–245. https://doi.org/10.1029/TC005i002p00227

Martin, A. K. (2006). Oppositely directed pairs of propagating rifts in back-arc basins: Double saloon door seafloor spreading during subduction rollback: OPPOSITE PAIRS OF PROPAGATING. Tectonics, 25(3), n/a-n/a. https://doi.org/10.1029/2005TC001885

Mascle, J., & Martin, L. (1990). Shallow structure and recent evolution of the Aegean Sea: A synthesis based on continuous reflection profiles. Marine Geology, 94(4), 271–299. https://doi.org/10.1016/0025-3227(90)90060-W

Mauffret, A., Lamotte, D. F. de, Lallemant, S., Gorini, C., & Maillard, A. (2004). E–W opening of the Algerian Basin (Western Mediterranean). Terra Nova, 16(5), 257–264. https://doi.org/10.1111/j.1365-3121.2004.00559.x

Mauffret, Alain. (2007). The Northwestern (Maghreb) boundary of the Nubia (Africa) Plate. Tectonophysics, 429(1), 21–44. https://doi.org/10.1016/j.tecto.2006.09.007

Medaouri, M. (2014). Origine de la segmentation de la marge algérienne et implications sur l'évolution géodynamique et des ressources pétrolières (Doctoral dissertation). Université de Bretagne occidentale, Brest, France. Retrieved from https://spiral.oca.eu/images/spiral/pdf/Mourad.pdf

Medaouri, M., Déverchère, J., Graindorge, D., Bracene, R., Badji, R., Ouabadi, A., et al. (2014). The transition from Alboran to Algerian basins (Western Mediterranean Sea): Chronostratigraphy, deep crustal structure and tectonic evolution at the rear of a narrow slab rollback system. Journal of Geodynamics, 77, 186–205. https://doi.org/10.1016/j.jog.2014.01.003

Michard, A., Chalouan, A., Feinberg, H., Goffé, B., & Montigny, R. (2002). How does the Alpine belt end between Spain and Morocco ? Bulletin de La Société Géologique de France, 173(1), 3–15. https://doi.org/10.2113/173.1.3

Michard, A., Negro, F., Saddiqi, O., Bouybaouene, M. L., Chalouan, A., Montigny, R., & Goffé, B. (2006). Pressure–temperature–time constraints on the Maghrebide mountain building: evidence from the Rif–Betic transect (Morocco, Spain), Algerian correlations, and geodynamic implications. Comptes Rendus Geoscience, 338(1), 92–114. https://doi.org/10.1016/j.crte.2005.11.011

Mihoubi, A., Schnürle, P., Benaissa, Z., Badsi, M., Bracene, R., Djelit, H., et al. (2014). Seismic imaging of the eastern Algerian margin off Jijel: integrating wide-angle seismic modelling and multichannel seismic pre-stack depth migration. Geophysical Journal International, 198(3), 1486–1503. https://doi.org/10.1093/gji/ggu179

Müller, R. D., Sdrolias, M., Gaina, C., & Roest, W. R. (2008). Age, spreading rates, and spreading asymmetry of the world's ocean crust. Geochemistry, Geophysics, Geosystems, 9(4). https://doi.org/10.1029/2007GC001743

Pellen, R., Aslanian, D., Rabineau, M., Leroux, E., Gorini, C., Silenziario, C., et al. (2016). The Minorca Basin: a buffer zone between the Valencia and Liguro-Provençal Basins (NW Mediterranean Sea). Terra Nova, 28(4), 245–256. https://doi.org/10.1111/ter.12215

Pelletier, B., Lafoy, Y., & Missegue, F. (1993). Morphostructure and magnetic fabric of the northwestern North Fiji Basin. Geophysical Research Letters, 20(12), 1151–1154. https://doi.org/10.1029/93GL01240

Piromallo, C., & Morelli, A. (2003). P wave tomography of the mantle under the Alpine-Mediterranean area. Journal of Geophysical Research: Solid Earth, 108(B2). https://doi.org/10.1029/2002JB001757

Platt, J. P., & Vissers, R. L. M. (1989). Extensional collapse of thickened continental lithosphere: A working hypothesis for the Alboran Sea and Gibraltar arc. Geology, 17(6), 540–543. https://doi.org/10.1130/0091-7613(1989)017<0540:ECOTCL>2.3.CO;2

Platt, John P., Anczkiewicz, R., Soto, J.-I., Kelley, S. P., & Thirlwall, M. (2006). Early Miocene continental subduction and rapid exhumation in the western Mediterranean. Geology, 34(11), 981–984. https://doi.org/10.1130/G22801A.1

Platt, John P., Behr, W. M., Johanesen, K., & Williams, J. R. (2013). The Betic-Rif Arc and Its Orogenic Hinterland: A Review. Annual Review of Earth and Planetary Sciences, 41(1), 313–357. https://doi.org/10.1146/annurev-earth-050212-123951

Poort, J., Lucazeau, F., Le Gal, V., Dal Cin, M., Leroux, E., Bouzid, A., et al. (2020). Heat flow in the Western Mediterranean: Thermal anomalies on the margins, the seafloor and the transfer zones. Marine Geology, 419, 106064. https://doi.org/10.1016/j.margeo.2019.106064

Recanati, A., Missenard, Y., Leprêtre, R., Gautheron, C., Barbarand, J., Abbassene, F., et al. (2019). A Tortonian onset for the Algerian margin inversion: Evidence from low-temperature thermochronology. Terra Nova, 31(1), 39–48. https://doi.org/10.1111/ter.12367

Rehault, J.-P., Boillot, G., & Mauffret, A. (1984). The Western Mediterranean Basin geological evolution. Marine Geology, 55(3), 447–477. https://doi.org/10.1016/0025-3227(84)90081-1

Richard, P. (1991). Experiments on faulting in a two-layer cover sequence overlying a reactivated basement fault with oblique-slip. Journal of Structural Geology, 13(4), 459–469. https://doi.org/10.1016/0191-8141(91)90018-E

Roca, E., & Guimerà, J. (1992). The Neogene structure of the eastern Iberian margin: Structural constraints on the crustal evolution of the Valencia trough (western Mediterranean). Tectonophysics, 203(1), 203–218. https://doi.org/10.1016/0040-1951(92)90224-T

Romagny, A., Jolivet, L., Menant, A., Bessière, E., Maillard, A., Canva, A., et al. (2020). Detailed tectonic reconstructions of the Western Mediterranean region for the last 35 Ma, insights on driving mechanisms. Bulletin de La Société Géologique de France, 191(37). https://doi.org/10.1051/bsgf/2020040

Rosenbaum, G., Lister, G. S., & Duboz, C. (2002). Reconstruction of the tectonic evolution of the western Mediterranean since the Oligocene. Journal of the Virtual Explorer, 08. https://doi.org/10.3809/jvirtex.2002.00053

Roure, F., Casero, P., & Addoum, B. (2012). Alpine inversion of the North African margin and delamination of its continental lithosphere. Tectonics, 31(3). https://doi.org/10.1029/2011TC002989

Royden, L.H. (1993). Evolution of retreating subduction boundaries formed during continental collision. Tectonics, 12(3), 629–638. https://doi.org/10.1029/92TC02641

Ryan, W.B.F., Carbotte, S. M., Coplan, J. O., O'Hara, S., Melkonian, A., Arko, R., et al. (2009). Global Multi-Resolution Topography synthesis. Geochemistry, Geophysics, Geosystems, 10(3). https://doi.org/10.1029/2008GC002332

Schellart, W.P., & Moresi, L. (2013). A new driving mechanism for backarc extension and backarc shortening through slab sinking induced toroidal and poloidal mantle flow: Results from dynamic subduction models with an overriding plate. Journal of Geophysical Research: Solid Earth, 118(6), 3221–3248. https://doi.org/10.1002/jgrb.50173

Schellart, W. P., Lister, G. S., & Jessell, M. W. (2002). Analogue modeling of arc and backarc deformation in the New Hebrides arc and North Fiji Basin. Geology, 30(4), 311–314. https://doi.org/10.1130/0091-7613(2002)030<0311:AMOAAB>2.0.CO;2

Schettino, A., & Turco, E. (2006). Plate kinematics of the Western Mediterranean region during the Oligocene and Early Miocene. Geophysical Journal International, 166(3), 1398–1423. https://doi.org/10.1111/j.1365-246X.2006.02997.x

Spakman, W., & Wortel, R. (2004). A Tomographic View on Western Mediterranean Geodynamics. In W. Cavazza, F. Roure, W. Spakman, G. M. Stampfli, & P. A. Ziegler (Eds.), The TRANSMED Atlas. The Mediterranean Region from Crust to Mantle: Geological and Geophysical Framework of the Mediterranean and the Surrounding Areas (pp. 31–52). Berlin, Heidelberg: Springer Berlin Heidelberg. https://doi.org/10.1007/978-3-642-18919-7_2

Speranza, F., Villa, I. M., Sagnotti, L., Florindo, F., Cosentino, D., Cipollari, P., & Mattei, M. (2002). Age of the Corsica–Sardinia rotation and Liguro–Provençal Basin spreading: new paleomagnetic and Ar/Ar evidence. Tectonophysics, 347(4), 231–251. https://doi.org/10.1016/S0040-1951(02)00031-8

Taylor, B., Zellmer, K., Martinez, F., & Goodliffe, A. (1996). Sea-floor spreading in the Lau back-arc basin. Earth and Planetary Science Letters, 144(1), 35–40. https://doi.org/10.1016/0012-821X(96)00148-3

Torsvik, T. H., & Cocks, L. R. M. (2016). Earth History and Palaeogeography. Cambridge: Cambridge University Press. https://doi.org/10.1017/9781316225523

Veeken, P. (2007). Seismic Stratigraphy, Basin Analysis and Reservoir Characterisation.

Vergés, J., & Fernàndez, M. (2012). Tethys–Atlantic interaction along the Iberia–Africa plate boundary: The Betic–Rif orogenic system. Tectonophysics, 579, 144–172. https://doi.org/10.1016/j.tecto.2012.08.032

Vila, J.M. (1980). La chaîne alpine d'Algérie orientale et des confins algéro-tunisiens (Doctoral dissertation). Université Pierre et Marie Curie (Paris VI), France.

Vine, F. J., & Matthews, D. H. (1963). Magnetic Anomalies Over Oceanic Ridges. Nature, 199(4897), 947–949. https://doi.org/10.1038/199947a0

Wallace, L. M., McCaffrey, R., Beavan, J., & Ellis, S. (2005). Rapid microplate rotations and backarc rifting at the transition between collision and subduction. Geology, 33(11), 857. https://doi.org/10.1130/G21834.1

Wortel, M., & Spakman, W. (2001). Subduction and Slab Detachment in the Mediterranean-Carpathian Region. Science, 291. https://doi.org/10.1126/science.290.5498.1910

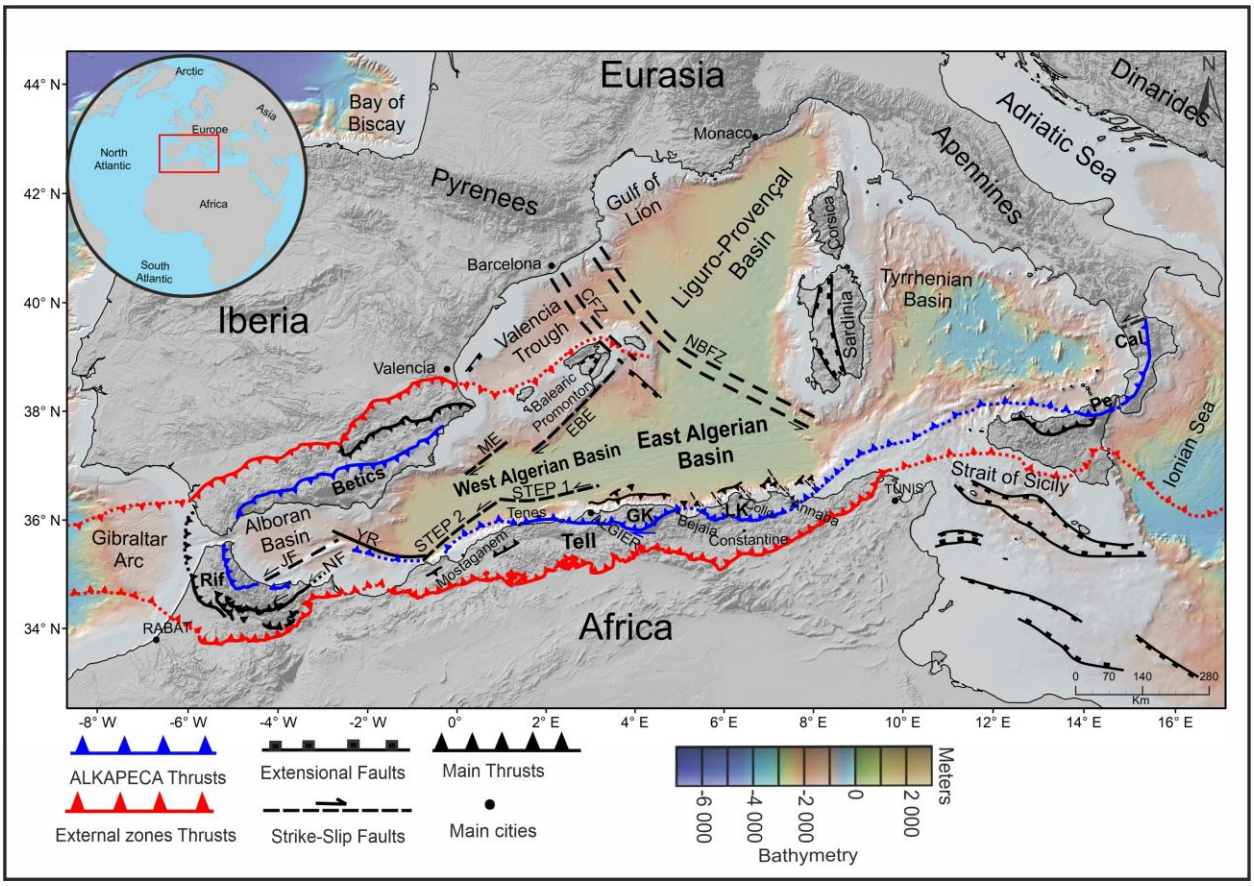
Eurasia
Africa
Iberia
Bay of Biscay
Pyrenees
Gulf of Lion
Liguro-Provençal Basin
Corsica
Sardinia
Tyrrhenian Basin
Apennines
Adriatic Sea
Dinarides
Ionian Sea
Monaco
Barcelona
Valencia
Valencia Trough
IST
NBFZ
Balearic Promontory
EBE
ME
Betics
West Algerian Basin
East Algerian Basin
STEP 1
STEP 2
Tenes
GK
Tell
Bejaia
Constantine
Collo
Annaba
TUNIS
Strait of Sicily
Alboran Basin
JF
NF
YR
Rif
Gibraltar Arc
RABAT
Mostaganem
Arctic
Europe
Asia
North Atlantic
Africa
South Atlantic
N
44° N
42° N
40° N
38° N
36° N
34° N
-8° W
-6° W
-4° W
-2° W
0°
2° E
4° E
6° E
8° E
10° E
12° E
14° E
16° E
0 70 140 280
Km
ALKAPECA Thrusts
External zones Thrusts
Extensional Faults
Strike-Slip Faults
Main Thrusts
Main cities
Meters
-6 000
-4 000
-2 000
0
2 000
Bathymetry

Figure 1

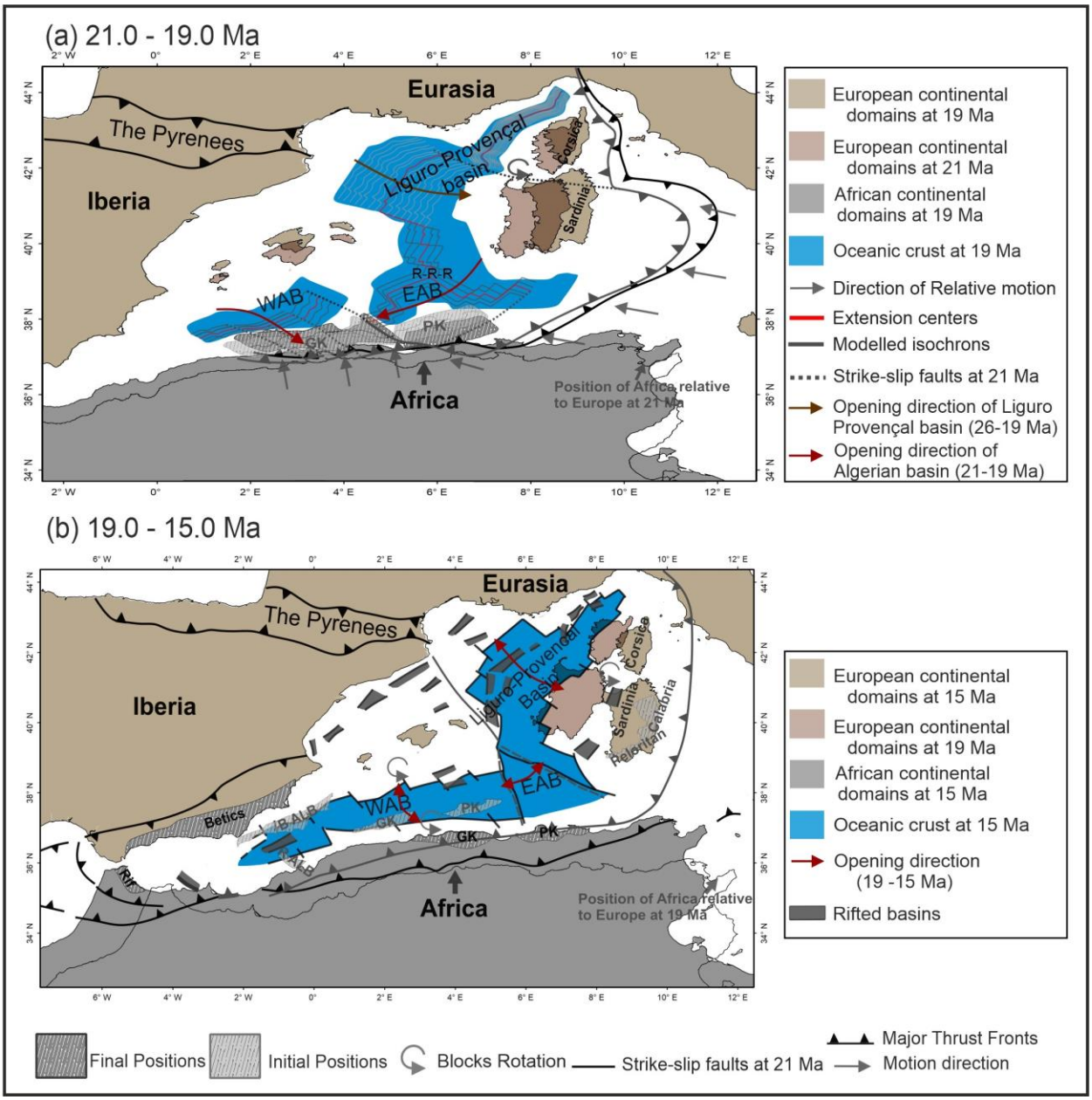
(a) 21.0 - 19.0 Ma
Eurasia
The Pyrenees
Iberia
Liguro-Provençal basin
Corsica
Sardinia
R-R-R
WAB
EAB
GK
PK
Africa
Position of Africa relative to Europe at 21 Ma
European continental domains at 19 Ma
European continental domains at 21 Ma
African continental domains at 19 Ma
Oceanic crust at 19 Ma
Direction of Relative motion
Extension centers
Modelled isochrons
Strike-slip faults at 21 Ma
Opening direction of Liguro Provençal basin (26-19 Ma)
Opening direction of Algerian basin (21-19 Ma)
(b) 19.0 - 15.0 Ma
Eurasia
The Pyrenees
Iberia
Liguro-Provençal Basin
Corsica
Sardinia
Peloritan
Calabria
Betics
Rif
WAB
EAB
GK
PK
Africa
Position of Africa relative to Europe at 19 Ma
European continental domains at 15 Ma
European continental domains at 19 Ma
African continental domains at 15 Ma
Oceanic crust at 15 Ma
Opening direction (19 -15 Ma)
Rifted basins
Final Positions
Initial Positions
Blocks Rotation
Strike-slip faults at 21 Ma
Major Thrust Fronts
Motion direction

Figure 2

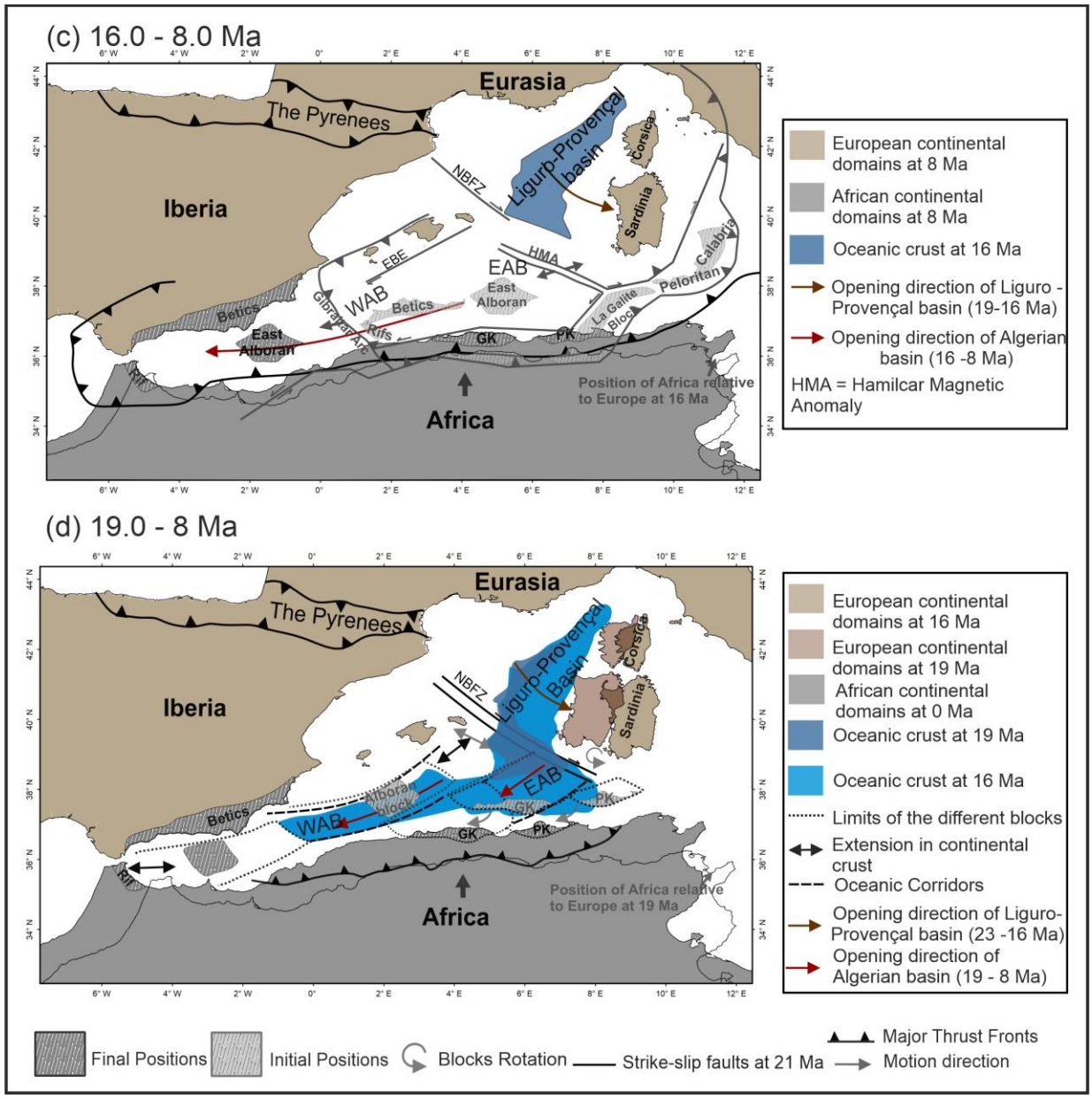
(c) 16.0 - 8.0 Ma
Eurasia
The Pyrenees
Iberia
Ligurb-Provençal basin
Corsica
Sardinia
NBFZ
EBE
HMA
EAB
East Alboran
WAB
Betics
Gibraltar Arc
Rifs
GK
PK
La Galite Block
Peloritan
Calabria
Africa
Position of Africa relative to Europe at 16 Ma
European continental domains at 8 Ma
African continental domains at 8 Ma
Oceanic crust at 16 Ma
Opening direction of Liguro - Provençal basin (19-16 Ma)
Opening direction of Algerian basin (16 -8 Ma)
HMA = Hamilcar Magnetic Anomaly
(d) 19.0 - 8 Ma
Eurasia
The Pyrenees
Iberia
Ligurb-Provençal Basin
Corsica
Sardinia
NBFZ
EAB
WAB
Alboran block
Betics
GK
PK
Rif
Africa
Position of Africa relative to Europe at 19 Ma
European continental domains at 16 Ma
European continental domains at 19 Ma
African continental domains at 0 Ma
Oceanic crust at 19 Ma
Oceanic crust at 16 Ma
Limits of the different blocks
Extension in continental crust
Oceanic Corridors
Opening direction of Liguro-Provençal basin (23 -16 Ma)
Opening direction of Algerian basin (19 - 8 Ma)
Final Positions
Initial Positions
Blocks Rotation
Strike-slip faults at 21 Ma
Major Thrust Fronts
Motion direction

Figure 2

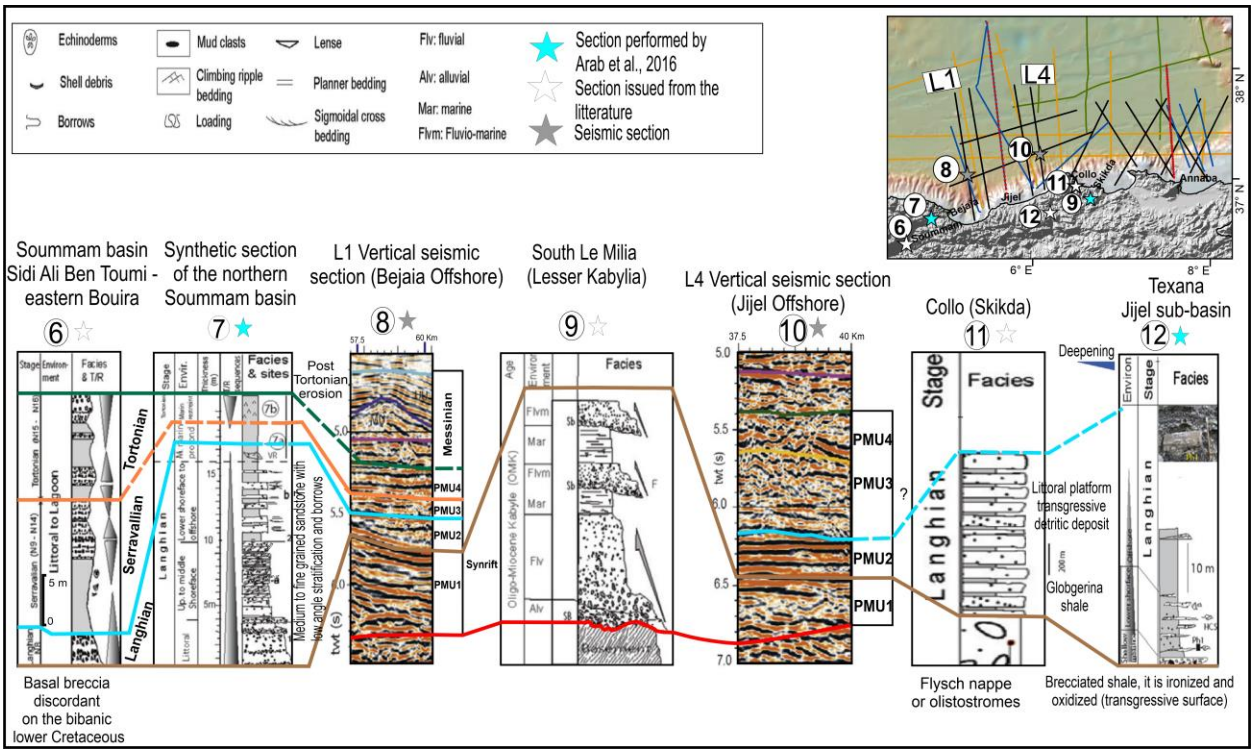

Figure 3

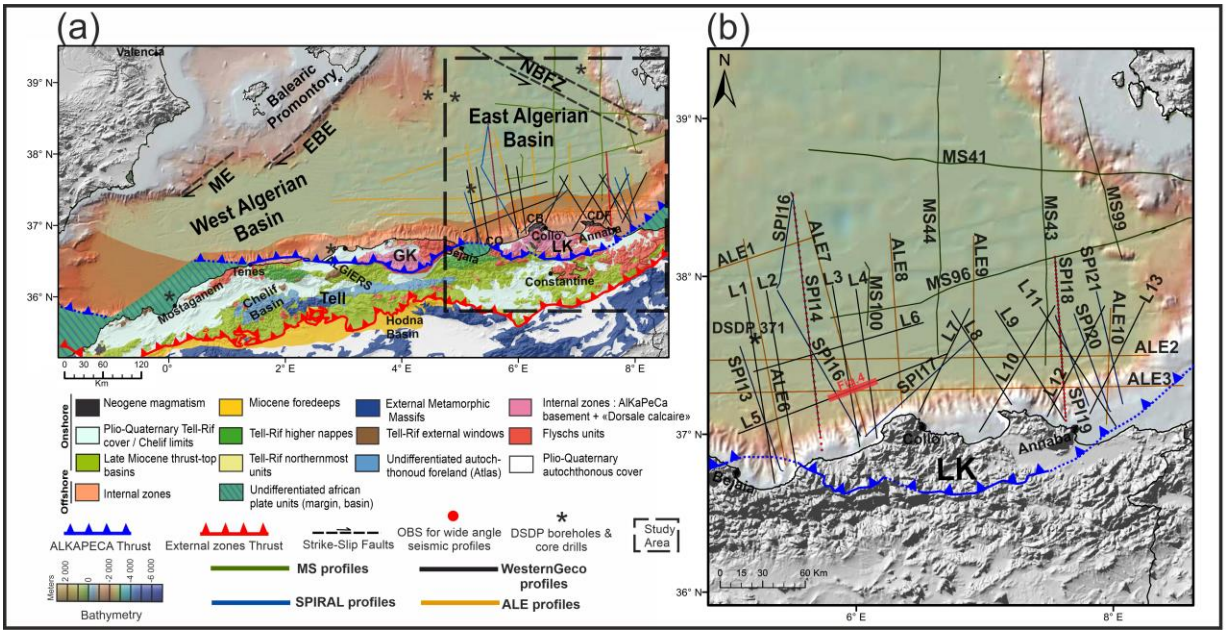

Figure 4

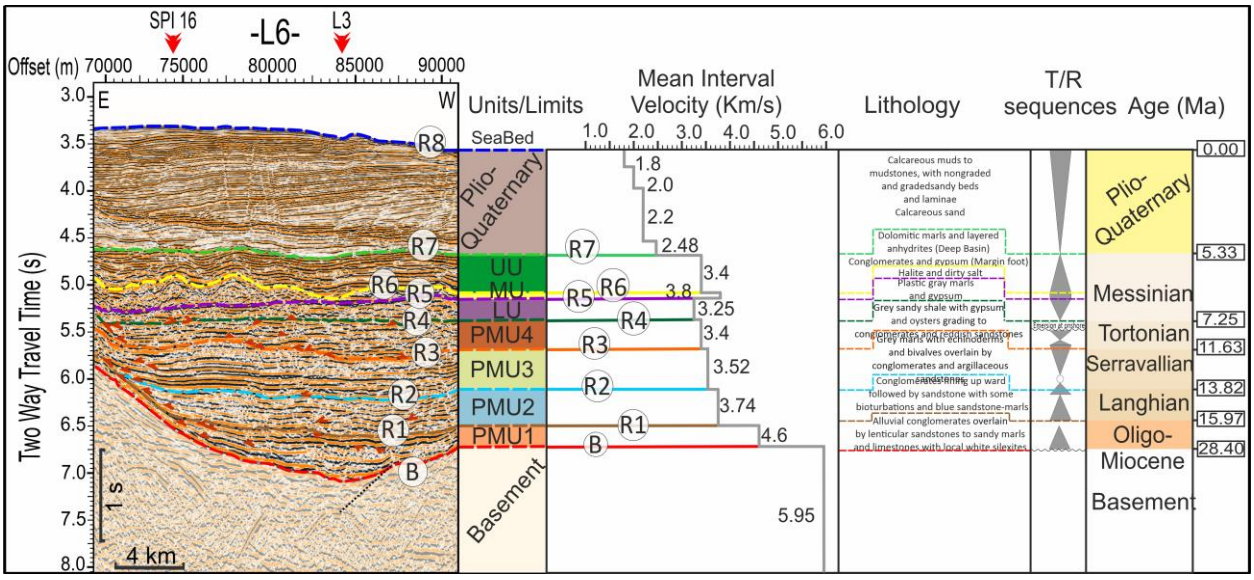

Figure 5

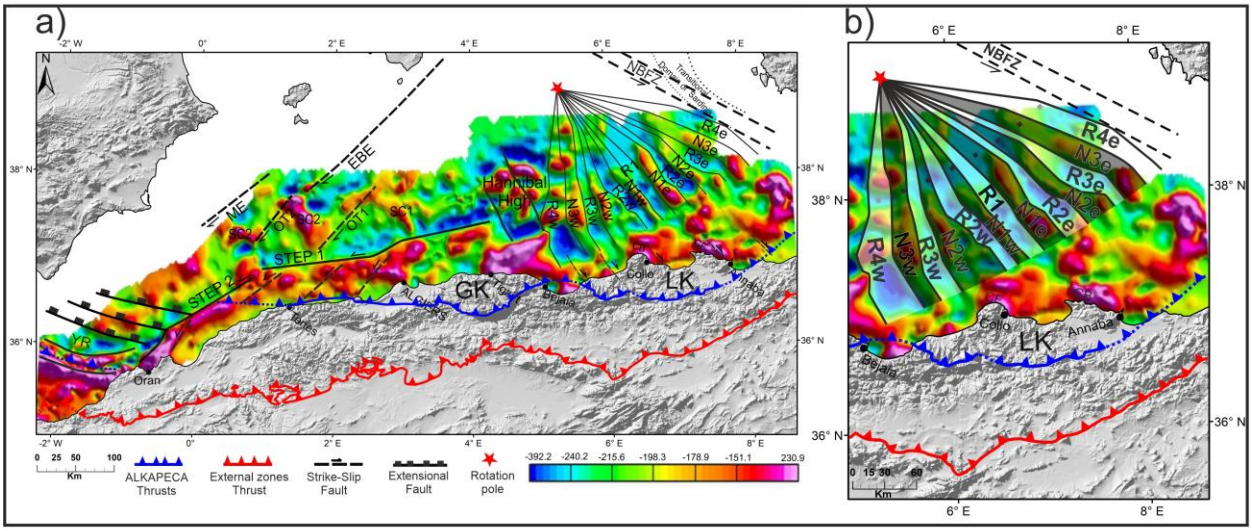

Figure 6

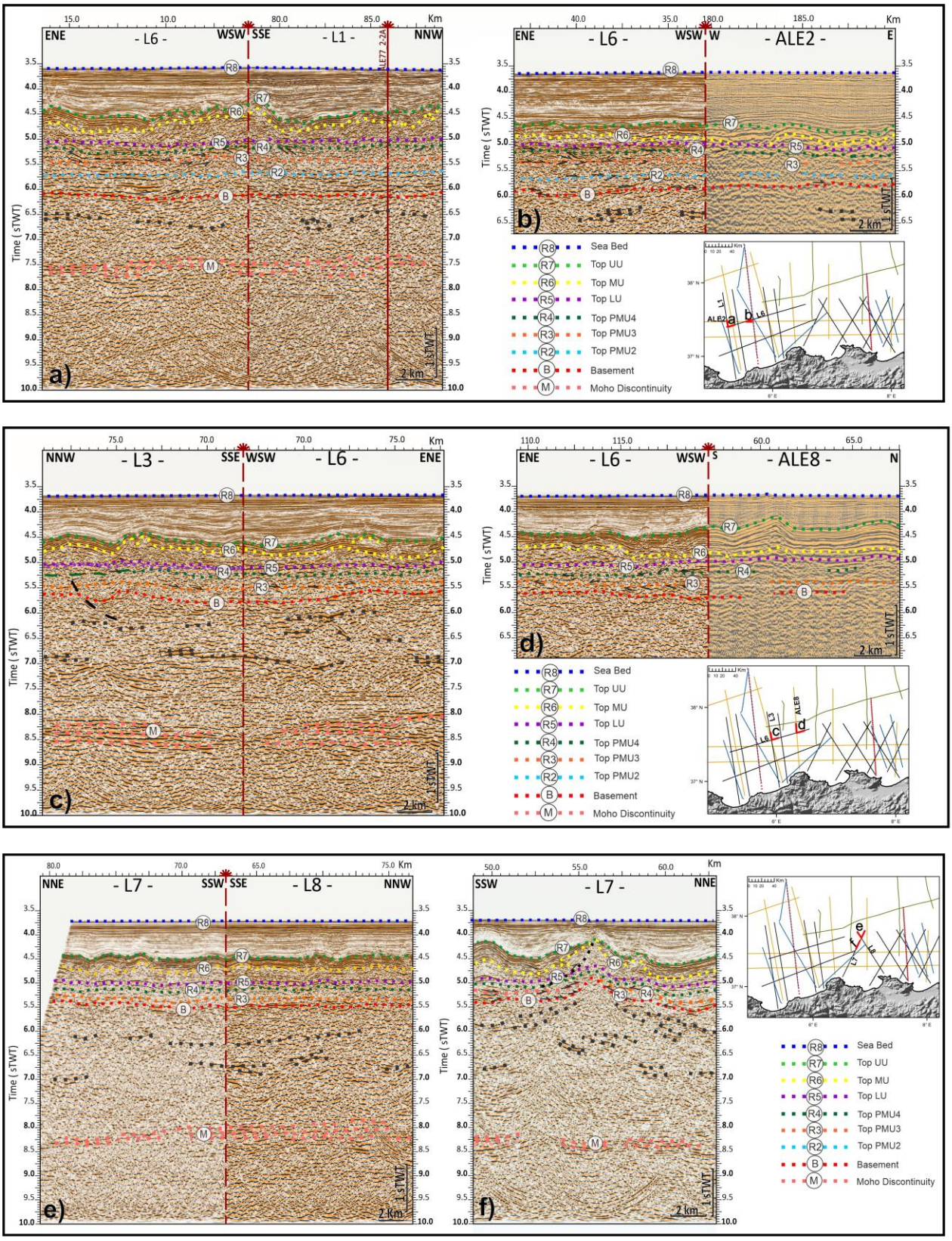
a)
b)
c)
d)
e)
f)
- L6 -
- L1 -
- ALE2 -
- L3 -
- L8 -
- L7 -
- ALE8 -
Time (sTWT)
Km
2 km
1 sTWT
Sea Bed
Top UU
Top MU
Top LU
Top PMU4
Top PMU3
Top PMU2
Basement
Moho Discontinuity

Figure 7

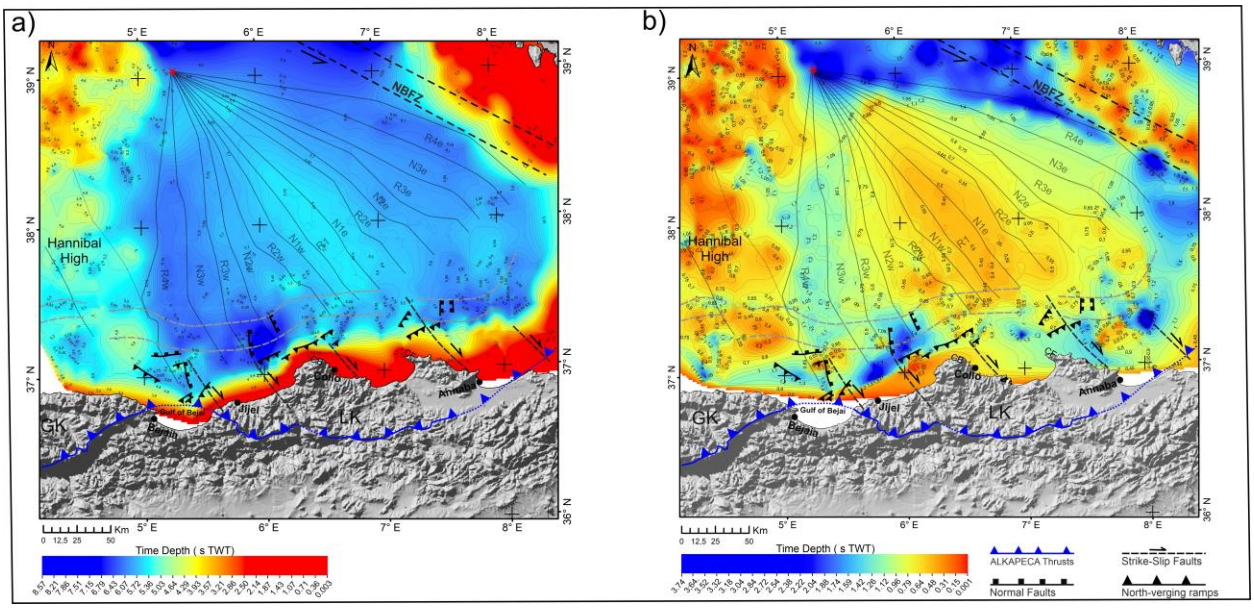
a)
b)
NBFZ
Hannibal High
GK
LK
Gulf of Bejai
Jijel
Collo
Annaba
Time Depth (s TWT)
ALKAPECA Thrusts
Normal Faults
Strike-Slip Faults
North-verging ramps

Figure 8

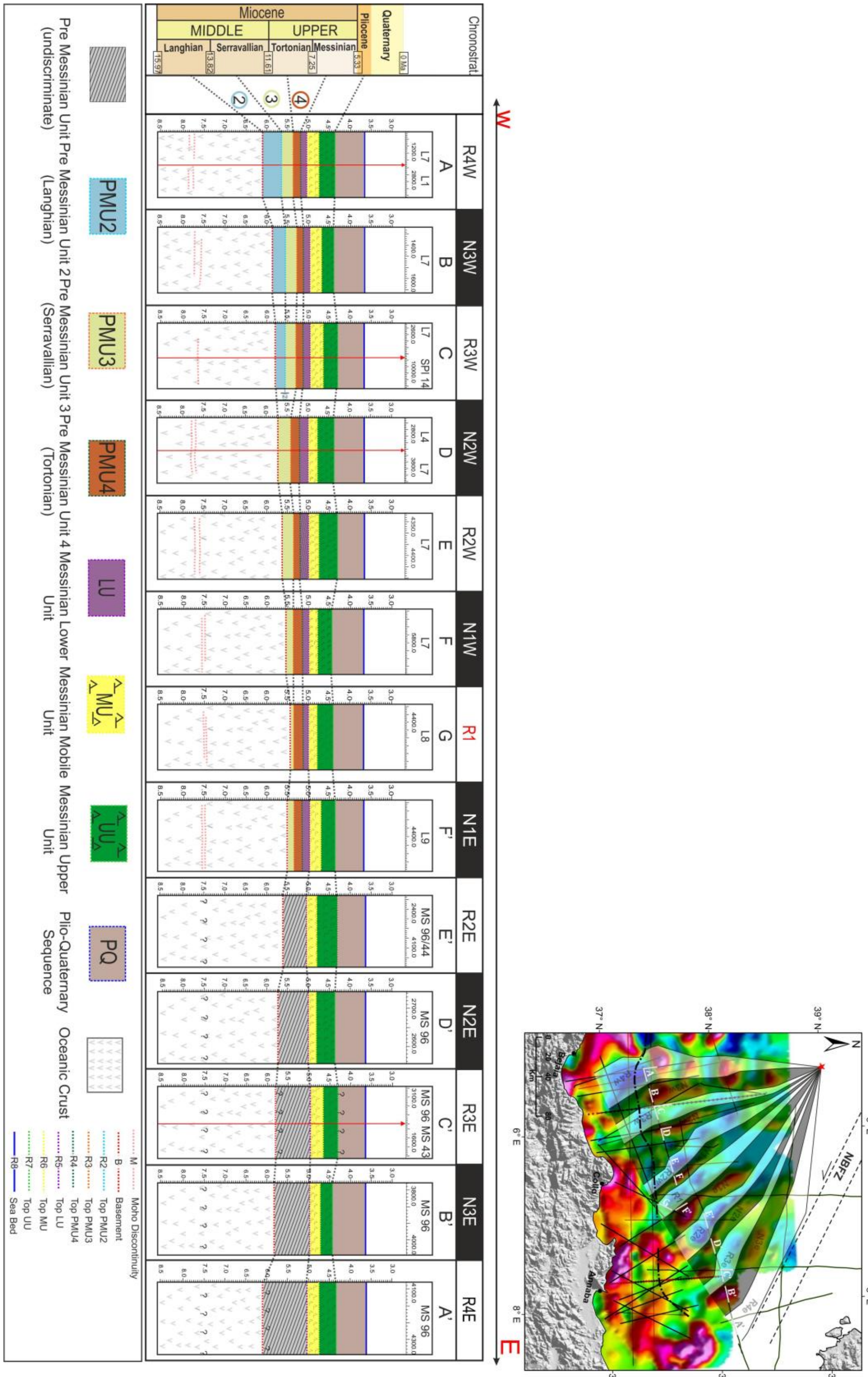
Chronostrat.
Miocene
MIDDLE
UPPER
Langhian
Serravallian
Tortonian
Messinian
Pliocene
Quaternary
W
E
R4W
N3W
R3W
N2W
R2W
N1W
R1
N1E
R2E
N2E
R3E
N3E
R4E
A
B
C
D
E
F
G
F'
E'
D'
C'
B'
A'
Pre Messinian Unit (undiscriminate)
PMU2
Pre Messinian Unit 2 (Langhian)
PMU3
Pre Messinian Unit 3 (Serravallian)
PMU4
Pre Messinian Unit 4 (Tortonian)
LU
Messinian Lower Unit
MU
Messinian Mobile Unit
UU
Messinian Upper Unit
PQ
Plio-Quaternary Sequence
Oceanic Crust
M Moho Discontinuity
B Basement
R2 Top PMU2
R3 Top PMU3
R4 Top PMU4
R5 Top LU
R6 Top MU
R7 Top UU
R8 Sea Bed
NBFZ
Collo
Annaba
37° N
38° N
39° N
6° E
8° E

Figure 9

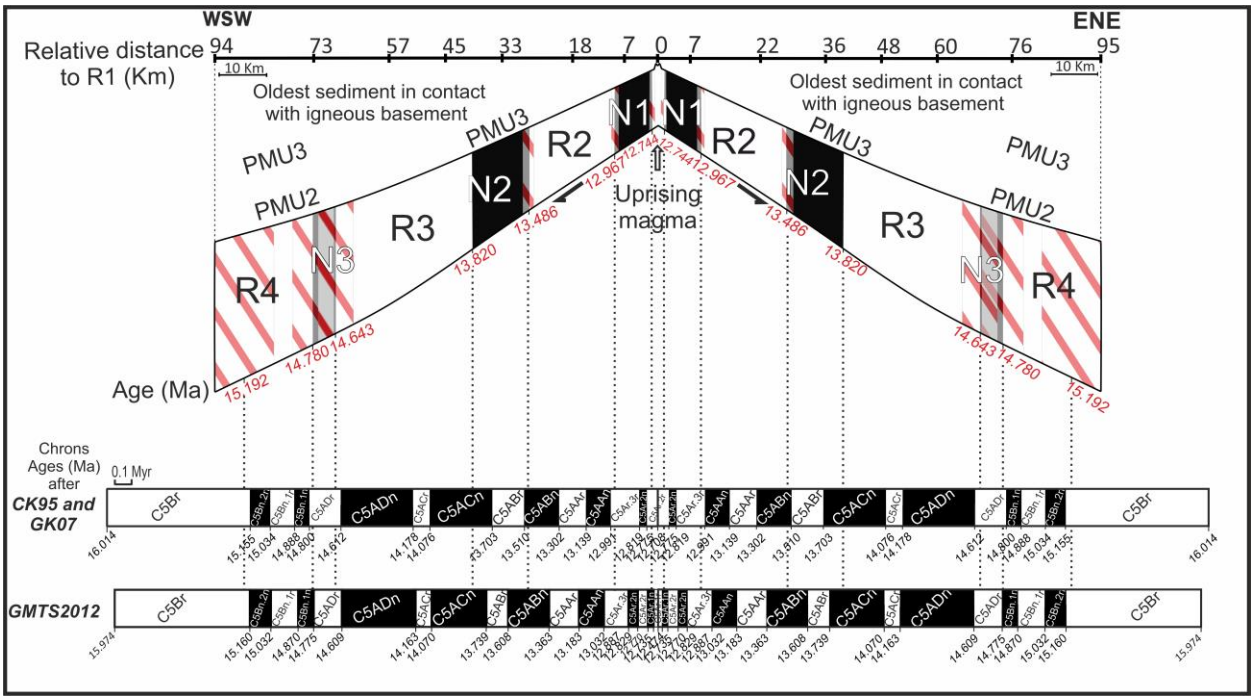
WSW
ENE
Relative distance to R1 (Km)
94 73 57 45 33 18 7 0 7 22 36 48 60 76 95
10 Km
10 Km
Oldest sediment in contact with igneous basement
Oldest sediment in contact with igneous basement
PMU3
PMU2
R4
N3
R3
N2
R2
N1
N1
R2
N2
R3
N3
R4
PMU3
PMU2
PMU3
12.967 12.744 12.744 12.967
13.486
13.820
13.820
13.486
Uprising magma
Age (Ma)
15.192 14.780 14.643
14.643 14.780 15.192
Chrons Ages (Ma) after
CK95 and GK07
0.1 Myr
GMTS2012
C5Br
C5ADn
C5ACn
C5ABn
C5AAn

Figure 10

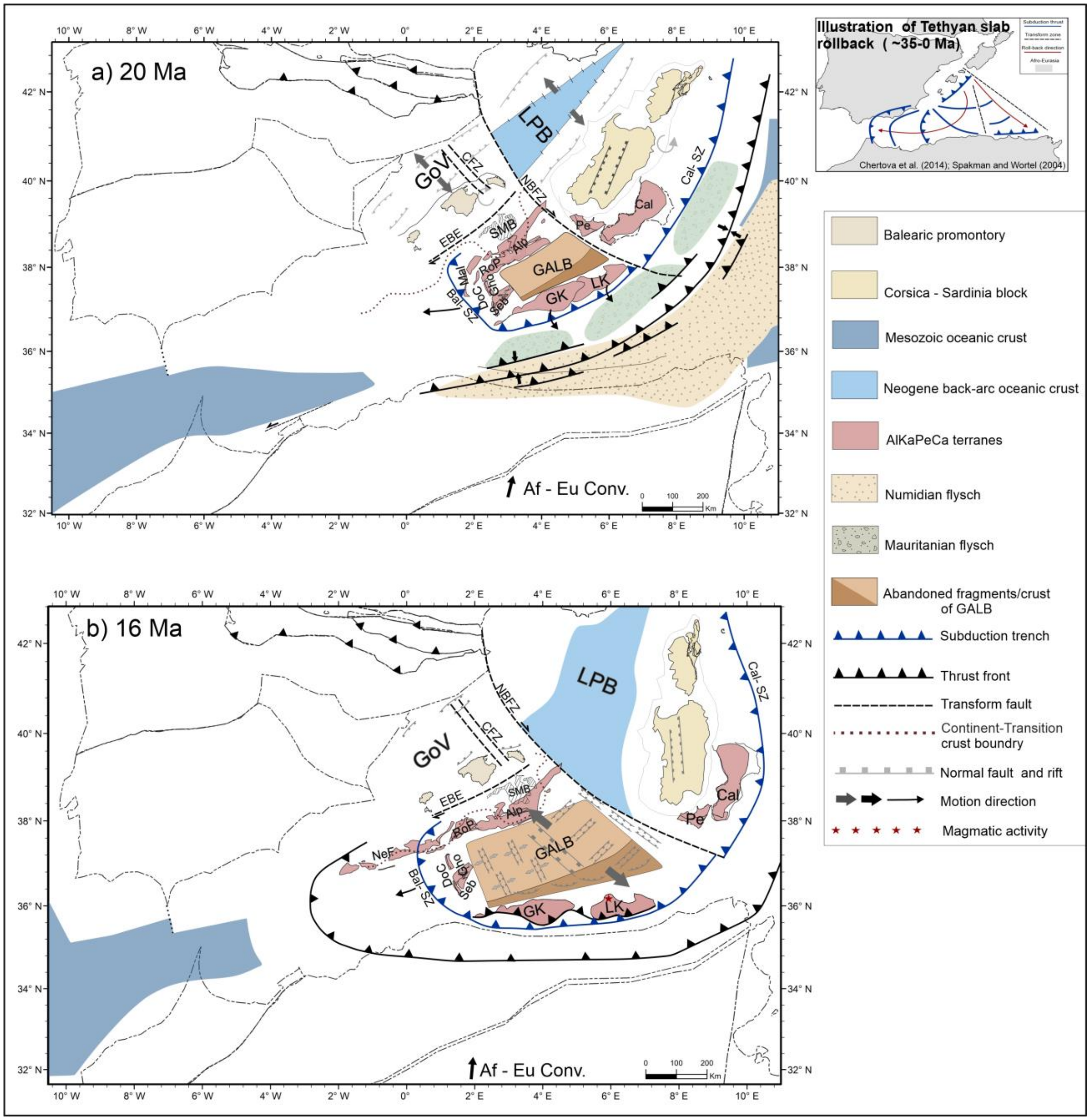
a) 20 Ma
b) 16 Ma
Illustration of Tethyan slab rollback (~35-0 Ma)
Chertova et al. (2014); Spakman and Wortel (2004)
Balearic promontory
Corsica - Sardinia block
Mesozoic oceanic crust
Neogene back-arc oceanic crust
AlKaPeCa terranes
Numidian flysch
Mauritanian flysch
Abandoned fragments/crust of GALB
Subduction trench
Thrust front
Transform fault
Continent-Transition crust boundry
Normal fault and rift
Motion direction
Magmatic activity
LPB
GoV
CFZ
NBFZ
EBE
SMB
Alp
RoP
GALB
GK
LK
Cal
Pe
Cal- SZ
Bal- SZ
DoC
Seb
NeF
Af - Eu Conv.

Figure 11

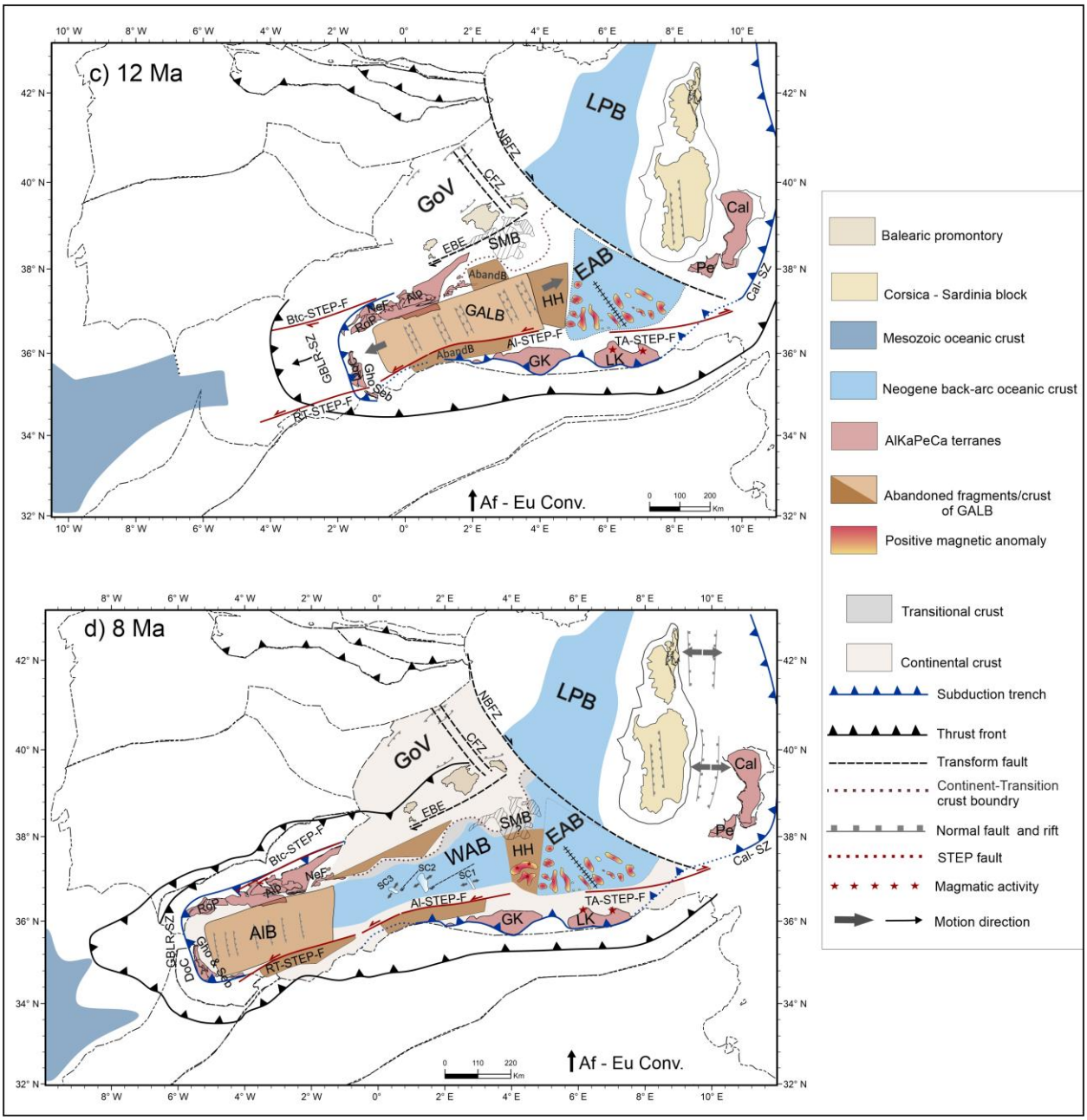
c) 12 Ma
d) 8 Ma
LPB
GoV
NBFZ
CFZ
EBE
SMB
EAB
HH
GALB
AbandB
AlKaPeCa
Btc-STEP-F
RT-STEP-F
Al-STEP-F
TA-STEP-F
GBLR-SZ
Cal-SZ
Cal
Pe
GK
LK
RGP
NeF
Alb
Gho & Sp
DoC
WAB
AlB
SC1
SC2
SC3
Af - Eu Conv.
Balearic promontory
Corsica - Sardinia block
Mesozoic oceanic crust
Neogene back-arc oceanic crust
AlKaPeCa terranes
Abandoned fragments/crust of GALB
Positive magnetic anomaly
Transitional crust
Continental crust
Subduction trench
Thrust front
Transform fault
Continent-Transition crust boundry
Normal fault and rift
STEP fault
Magmatic activity
Motion direction

Figure 11